THE JOURNAL OF PHYSICAL CHEMISTRY B
A JOURNAL OF THE AMERICAN CHEMICAL SOCIETY

pubs.acs.org/JPCB

Article

Importance of Experiments That Can Test Theories Critically

Published as part of The Journal of Physical Chemistry B special issue "Mark Ediger Festschrift".

K. L. Ngai*

Cite This: *J. Phys. Chem. B* 2024, 128, 10709−10726

Read Online

ACCESS | Metrics & More | Article Recommendations | Supporting Information

ABSTRACT: General dynamic and thermodynamic properties of complex materials, including amorphous polymers and molecular glass-formers, have been established from the wealth of experimental data accumulated over the years. Naturally, these general properties attract researchers to construct theories and models to address and explain them. Often more than one theory with contrasting or even conflicting theoretical bases can equally explain a general property rather well. The correct explanation becomes unclear, and progress is stopped. The resolution of the problem comes when an innovative experiment is performed with insightful results that can critically test the premise and assumptions of each theory. This important role played by experimentalists is exemplified by the contributions of Mark Ediger in several general properties considered in this paper: (1) dynamics of the components in binary polymer blends; (2) breakdown of the Stokes−Einstein and the Debye−Stokes−Einstein relations; (3) enhancement of surface mobility and in relation to formation of ultrastable glasses; and (4) the Johari−Goldstein β-relaxation in ultrastable glasses. Different theories proposed to explain these properties are discussed, including the Coupling Model of the author.

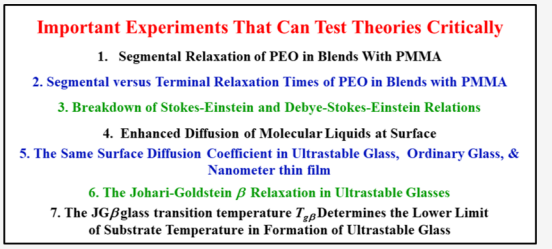

INTRODUCTION

In scientific research, experimental studies have notable impacts by discovering new effects and phenomena or by producing novel data that can critically test the predictions of theories. These important roles played by experiments are most relevant in the research areas of relaxation and diffusion processes in complex materials, where diverse theories have been proposed. Studied by experimentalists and theorists from various disciplines, these are varieties of dynamic processes in widely different classes of materials. A huge amount of experimental data and simulation results has accumulated over the past several decades. It is important to distinguish those that are critical and essential to the construction of any viable theory with far-reaching applications. The experimental research performed by Mark Ediger over the years has produced key results in several areas crucial for any theory at least to be consistent with, and better to be able to explain quantitatively. Based on my experience, I can recall some critical experiments contributed by him in four different areas: (1) component dynamics of binary polymer blends[1−9]; (2) breakdown of the Debye−Stokes−Einstein relation[9−20]; (3) surface diffusion[21−28]; and (4) the Johari−Goldstein β-relaxation in ultrastable glass.[29] His studies are beneficial in particular for the development of my theoretical model of cooperative relaxation and diffusion in complex materials, i.e. the Coupling Model (CM).[30−32] In this paper, I revisit some of his important experimental data within the areas of (1)−(4), in conjunction with those related results of others. The comparisons of his data and related ones from others with the predictions of the CM are pointed out to demonstrate the impact of the former on the latter and vice versa. These important experimental research results of Ediger, emphasized in this study as a tribute to his scientific accomplishments, should be recognized as critical by others and addressed by any theory concerned with the relaxation and diffusion in complex materials. Various theories from other workers to explain his experimental data are discussed, highlighting the key differences in the treatments and the disagreements between them.

NMR SEGMENTAL RELAXATION OF D4PEO IN BLENDS WITH PMMA

The dynamics of the components in binary polymer blends is a research area in which Ediger and collaborators have made many valuable contributions. Some of his publications are cited herein.[1−9] There are research by others[33−58] with results having connections with those by him. Composed of two components with the glass transition temperatures T_{g1} of the slow component much higher than that *of* T_{g2} of the fast component, the highly asymmetric polymer blends (HAPB) exhibit anomalous dynamics properties in the segmental α-relaxation as well as the chain relaxation of the fast component in the blends not found when it is pure. When the low-T_g polymer is the minor

Received: May 28, 2024
Revised: September 17, 2024
Accepted: September 18, 2024
Published: October 16, 2024

component in the blend, experiments, and simulations of HAPB have found anomalous properties in both the segmental α-relaxation and the chain dynamics, not seen before in blends with smaller ΔT_g. These properties are likely caused by the enhanced dynamic constraint and stronger intermolecular interaction imposed by the much slower host. A review of the various anomalous properties was given in ref 59, where the Coupling Model (CM) was applied to explain the nine anomalous properties. In this tribute to Ediger chosen is the anomalous property found by him and his collaborators.[4] It is the insensitivity of segmental relaxation of the low-T_g poly(ethylene oxide) d4PEO to blend composition in blends with poly(methyl methacrylate) PMMA found in high Larmor frequency (46 and 76 MHz) deuteron NMR experiment by Lutz et al.[4] and also by Latique et al.,[35] where the segmental times $\tau_{\alpha,\mathrm{PEO},x}(T)$ of PEO in the blends are shorter than 1 ns. Similar results were found in other polymer blends including PEO with poly(vinyl acetate)[6] and hence the property is general.

High-molecular-weight miscible blends of PEO with poly(methyl methacrylate) PMMA, xPEO/$(1-x)$PMMA, are extreme cases of HAPB with the difference in the glass transition temperatures of the two polymers before mixing, $\Delta T_g = (T_{g1} - T_{g2})$, close to 200 K. The deuteron NMR experiments found the segmental relaxation times, $\tau_{\alpha,\mathrm{PEO},x}(T)$, of the fast perdeuerio-poly(ethylene oxide) d4PEO component in the range, $-8.5 \geq \log(\tau_{\alpha,\mathrm{PEO},x}(T)\ /\mathrm{s}) \geq -11.5$, are nearly independent of composition for blends from 3 to 30% d_4PEO over the temperature regime studied, and $\tau_{\alpha,\mathrm{PEO},x}(T)$ is not much longer than that of pure PEO.[4,35] This is shown in Figure 1. For example, $\tau_{\alpha,\mathrm{PEO},x}(T)$ is retarded by less than 1 order of magnitude in blends of 0.5% and up to 3% PEO content. The result holds for a wide range of temperatures extending to well below the glass transition temperature T_{g1} of the PMMA component. At T_{g1} the segmental relaxation times of PMMA are about 12 orders of magnitude longer than the $\tau_{\alpha,\mathrm{PEO},x}$ of PEO. The VFT fits of the data of $\tau_{\alpha,\mathrm{PEO},x}(T)$ in 3, 10, and 30% d_4PEO blends are shown by lines in Figure 1. Similar anomalous behavior is observed by deuteron NMR in PEO blends with polyvinyl acetate,[6] where the segmental dynamics of PEO are 9 orders of magnitude faster than the PVAc segmental dynamics for a 2% PEO blend near the T_{g1} of the PVAc component. In the range $-9 \geq \log(\tau_{\alpha,\mathrm{PEO},x}/\mathrm{s}) \geq -11.8$, the $\tau_{\alpha,\mathrm{PEO},x}(T)$ of PEO in 2% PEO blend differs from that in 50% PEO and 100%PEO blends by about half a decade and one decade, respectively. Thus, the d4PEO segmental dynamics are nearly independent of composition for blends from 0.5 to 30% d4PEO. At the lowest concentration of d4PEO studied, the blend is a dilute solution. This led Lutz et al.[4] to exclude intermolecular composition fluctuations as an explanation for the unusually fast d4PEO dynamics in the blends.

The findings by Lutz et al.[4] of the extremely fast PEO segmental dynamics in blend with poly(methyl methacrylate) have attracted attention. Various explanations of the origin of the anomaly were given,[4−7] and the Lodge−McLeish (LM) model[60] based on the self-concentration effect (the enhanced local concentration due to chain connectivity) was used. The CM[45,48] offered a different explanation. The explanations offered and the theories used to explain the data from the works by Ediger and co-workers[4,6] are discussed in the following subsections.

CM Explanation. This anomalously fast PEO segmental dynamics found by ^{2}H NMR measurements at 76 MHz (~2.1 ns) is particularly and naturally connected to the CM because

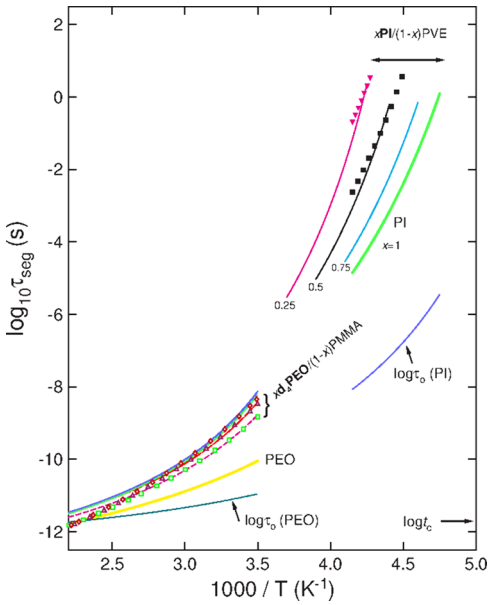

Figure 1. Segmental relaxation times for PEO neat (bold solid yellow line) and in blends with PMMA (lines) containing 3 to 30% PEO (from top to bottom) taken from the VFT fits of Lutz et al.[4] The most probable relaxation times are also shown, as calculated from eq 2 for the lower (□, $n = 0.76$), midrange (△, $n = 0.75$) and higher concentrations of PEO (◊, $n = 0.715$), respectively. Also shown is the independent relaxation time for PEO (dotted line, using $n = 0.5$), which lies close to $t_c = 2$ ps. Results are shown for PI neat (bold green line) and in blends with PVE containing 25 to 75% PI (lines), together with the calculated τ_{seg} for 25% (▼) and 50% (■) compositions. Note that the independent relaxation time for PI (dotted line) is four or more decades longer than t_c. Adapted with permission from ref 45. Copyright 2003 American Chemical Society.

the crux of CM explanation given[45,48] is the basic premise of the CM. That is the universal crossover from the primitive relaxation with correlation function, $\phi(t) = \exp(-t/\tau_0)$ to the Kohlrausch relaxation with $\phi(t) = \exp[-(t/\tau)^{1-n}]$ at $t_c = 1-2$ ps for polymers.[31,32] It was verified by neutron scattering experiments on xPEO/$(1-x)$PMMA blends with $x = 10$, 20, 30, and 100% performed by Sakai et al.[43,44,57,58] to be discussed in Section 2.2, and by others in homopolymers.[60−63] The cross-over at t_c leads to the CM signature eq 1, which is applicable to various processes including the local segmental α-relaxation,[31,32]

$$\tau = [t_c^{-n}\tau_0]^{1/(1-n)} \tag{1}$$

The nearly independence of composition of d4PEO segmental dynamics in blends from 0.5 to 30% of d4PEO in blends with PMMA follows as consequences of the CM eq 1[45] when rewritten in the form

$$\tau_{\alpha,\mathrm{PEO},x}(T)/\tau_0(T) = [\tau_0(T)/t_c]^{n_\alpha/(1-n_\alpha)} \tag{2}$$

The primitive relaxation times $\tau_0(T)$ calculated from the deuteron $\tau_\alpha(T)$ of pure PEO ($x = 1$) by eq 2 in the temperature range of the d_4PEO deuterium NMR measurements are very short, ranging from 10^{-12} to 2×10^{-11} s. It is represented by the blue line in the lower part of Figure 1. Since $t_c = 1-2 \times 10^{-12}$ s determined by neutron scattering for polymers,[43,44,57] the ratio τ_0/t_c in eq 2 ranges from 1 to 5 as can be seen in Figure 1, and also $[\tau_0(T)/t_c]^{n_\alpha/(1-n_\alpha)}$ is not large and insensitive to variation of n_α with composition. Hence $\tau_{\alpha,\mathrm{PEO},x}(T)/\tau_0(T)$ do not vary much with the change of composition. This is further demonstrated by

https://doi.org/10.1021/acs.jpcb.4c03520
J. Phys. Chem. B 2024, 128, 10709−10726

actually calculating $\tau_{\alpha,\mathrm{PEO},x}(T)$ with values of n_α by eq 2 within the range suggested by the deuteron NMR experiment for different x values as shown by the smaller symbols in Figure 1.

On the other hand, had τ_0 been much longer than t_c, the $\tau_{\alpha,\mathrm{PEO},x}(T)$ predicted from eq 2 would be much longer than that of neat PEO, and strongly dependent on composition. This scenario is exemplified by other polymer blends such as 1,4-polyisoprene (PI) mixed with poly(vinylethylene) (PVE)[45−48] in Figure 1. In these other blends, neither the observed nor the calculated component dynamics behave like d_4PEO in PMMA because the experiments were carried out under conditions that the segmental dynamics of the neat lower-T_g polymer PI are much slower than that of d_4PEO in the deuterium NMR work,[4] and the corresponding τ_0 is much longer than t_c shown by another blue line in the middle of Figure 1.[45] As pointed out above, from eq 2 the factor determining how rapidly the segmental relaxation time τ_α of the faster component changes with composition is the ratio of its τ_0 in the blend ($\approx\tau_0$ in the pure state) to $t_c \approx 2$ ps. It is obvious from Figure 1 that τ_0 of PI is much longer than t_c, and thus the ratio $\tau_0(T)/t_c$ is much larger. Again by the CM eq 2, the much larger value of $\tau_0(T)/t_c$ is responsible for the large change of PI component $\tau_{\alpha,\mathrm{PI},x}(T)$ with x in the blends with PVE shown in Figure 1, in contrast to the near independence of the d4PEO dynamics to composition in blends with PMMA.

Support from Quasielastic Neutron Scattering Experiments. The 2003 paper on deuterium NMR segmental relaxation of d4PEO in blends with PMMA by Ediger and co-workers had an impact not only on the CM as described above, but also motivated Sakai, Maranas, and co-workers[43,44,57] to perform quasielastic neutron scattering (QENS) experiment on xPEO/$(1-x)$PMMA blends with x = 10, 20, 30, and 100%. The QENS results are shown in Figure 2 from ref 59 and compared with the deuteron NMR data of Lutz et al. The dynamics of the PEO component were determined over spatial scales from 3 to 10 Å. The QENS data not only support the CM explanation of the deuteron NMR data made in the 2004 paper,[45] but also provide solid evidence for the existence of the primitive relaxation time $\tau_0(T)$ of the PEO component. In fact, as shown in Figure S1 of the Supporting Information (SI), the QENS data taken in the picosecond-nanosecond time range reveal the crossover from a fast (f) primitive relaxation of the PEO component to a slow (s) Kohlrausch relaxation near t_c = 1 ps, close to t_c = 2 ps assumed in the 2004 paper. The relaxation times, $\tau_{\mathrm{QENS,f}}(T)$ and $\tau_{\mathrm{QENS,s}}(T)$, of the f- and the s-relaxations of PEO respectively obtained from QENS by Sakai et al. for pure PEO and PEO in blends with 10, 20, and 30% PEO at momentum transfer Q = 1.3 Å^{-1} are shown in Figure 2 by the larger size closed and open symbols, respectively. Comparisons are made there with $\tau_{\alpha,\mathrm{PEO},x}(T)$ from deuteron NMR (only the VFT fits data are shown by the lines), and the calculated $\tau(T)$ by the CM equation (small size symbols). As can be seen by inspection of the main figure as well as the upper inset, $\tau_{\mathrm{QENS,f}}(T)$ is insensitive to blending with PMMA, exactly the same as assumed for $\tau_0(T)$ in the 2004 paper.[45] The temperature dependence of $\tau_{\mathrm{QENS,f}}$ is Arrhenius with an activation energy of 10−15 kJ/mol, independent of composition and scattering vector Q, consistent with conformational transitions in PEO.[64] The Q-dependence of $\tau_{\mathrm{QENS,f}}$ is a power law $Q^{-\lambda}$ with λ varying between 2.0 and 2.5. Exponential correlation function, $\exp(-t/\tau_0)$, has $\tau_0 \propto Q^{-\lambda}$ with λ = 2.0. All these properties of $\tau_{\mathrm{QENS,f}}$ are indications that the fast process is the one-body independent or primitive relaxation time τ_0 of the CM.

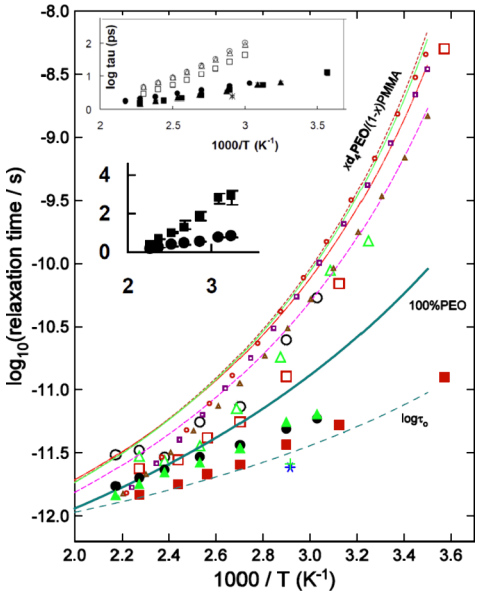

Figure 2. Comparing the Deuteron NMR and QENS data of PEO−PMMA blends. The large open and closed symbols are the relaxation times of the *slow* and *fast* processes respectively found by QENS experiments of Sakai et al.[43,44] at Q = 1.3 Å^{-1}. Dark blue circles for 10%, green triangles for 20%, red squares for 30% and + and * for 100% PEO. The upper inset shows by solid symbols the QENS relaxation times, $\tau_{\mathrm{QENS},\beta}$ of the *fast* process of PEO at Q = 1.3 Å^{-1} as a function of 1000/T: (●) 10%, (▲) 20%, (■) 30% and (×) 100%. Empty symbols correspond to the deuteron NMR segmental relaxation times: (○) 10%, (△) 20% and (□) 30%. The lower inset shows $\log(\tau_{\mathrm{QENS,s}})$ for the *slow* process (■) and $\log(\tau_{\mathrm{QENS,f}})$ for the *fast* process (●) of PEO in the 20% blend from QENS at Q = 1.3 Å^{-1} plotted against 1000/T. The units of the x-axis and y-axis in both insets are K^{-1} and ps, respectively. Also shown are the VFT fits to the deuteron NMR segmental relaxation times for pure PEO (bold blue solid line) and in blends with PMMA containing from 3% up to 30% PEO (upper thin lines from top to bottom) reported by Lutz et al.[4] The actual data are not shown to avoid crowding. Shown by the blue dashed-dotted line at the bottom is the primitive relaxation time $\tau_0(T)$ of neat PEO calculated by using n = 0.50. The small size symbols on top are the most probable relaxation times calculated for the 3% (○), 10% (□), and 30% (△) PEO blends with $\hat{n}$ = 0.76, 0.75, and 0.715, respectively.[45] Reproduced with permission from ref 59. Copyright 2013 American Institute of Physics.

The slow QENS relaxation time $\tau_{\mathrm{QENS,s}}(T)$, is slightly shorter than $\tau_{\alpha,\mathrm{PEO},x}(T)$ from deuteron NMR,[4] but their temperature dependences are similar except at very short times. Actually, the QENS data of $\tau_{\mathrm{QENS,s}}(T)$ should be more accurate than NMR data in the short time range because the highest frequency in NMR measurement is 76 MHz corresponding to $10^{-8.7}$ s. Remarkably, the value of $n \approx 0.5$ equivalent to the experimental value of the stretch exponent, $(1-n) \equiv \beta_K \approx 0.5$, for pure PEO, and $n \approx 0.75$ from $(1-n) \approx 0.25$ for 20% PEO from QENS experiments is close to the values used in the 2004 CM paper[45] to calculate $\tau_{\alpha,\mathrm{PEO},x}(T)$ by the CM equation. Notwithstanding, it is possible that the actual coupling parameter n of pure PEO in the ps-ns range is not as large as 0.50 as obtained directly from the stretch exponent $(1-n) \approx 0.50$ of Kohlrausch function used to fit the QENS and the deuteron NMR data.

Of special interest here is the insensitivity of the relaxation time $\tau_{\mathrm{QENS,s}}$ of the slow (S) QENS process to compositions of the three blends studied (see Figure 2). As seen before in the deuteron NMR experiment,[4] this is an anomalous behavior of the PEO/PMMA blends dynamics. However, now, the primitive

https://doi.org/10.1021/acs.jpcb.4c03520
J. Phys. Chem. B 2024, 128, 10709−10726

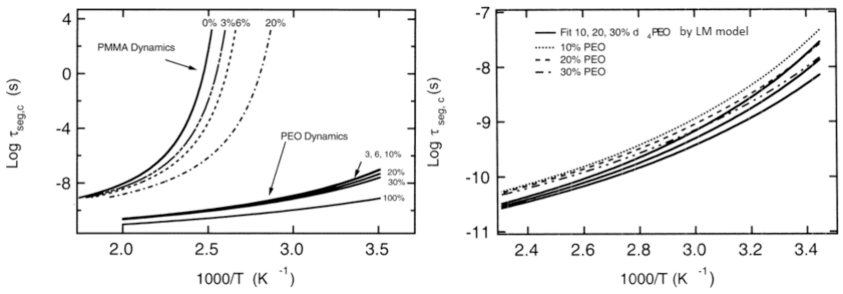

Figure 3. (Left) Segmental correlation times for both components in d4PEO/PMMA blends at various compositions. Solid lines for d4PEO are the result of fits of experimental data to the ϕ_{KWW} function with a VFT temperature dependence. Pure PMMA (labeled 0% meaning 0% d4PEO is present) dynamics are the VFT fit from dielectric relaxation measurements. PMMA dynamics in blends containing 3, 6, and 20% d4PEO were predicted assuming that PMMA dynamics are reflective of the blend T_g and that PMMA maintains a VFT temperature dependence in the blends. A 12 orders of magnitude segmental dynamic difference exists between PEO and PMMA segmental dynamics at the blend T_g for a 3% blend. PEO has a very weak composition dependence over the temperature regime studied. (Right) Lodge−McLeish fit of d_4PEO segmental correlation times for d_4PEO/PMMA blends of 10, 20, and 30% d_4PEO. One parameter, ϕ_{self}, was varied in the fitting; the best fit was obtained with $\phi_{self} = 0.57$. The blend T_g was predicted by using the Fox equation. Reproduced with permission from ref 4. Copyright 2004 American Chemical Society.

relaxation of the CM has been identified with the fast (f) relaxation seen by QENS, and its cross-over to the slow many-body relaxation has been observed in the QENS experiment by the cross-over from the f-process to the s-process. Therefore, $\tau_{QENS,s}(T)$ and $\tau_{QENS,f}(T)$ obey the CM eq 1, after substituting therein τ by $\tau_{QENS,s}$ and τ_0 by $\tau_{QENS,f}$. Moreover, the ratio, $\tau_{QENS,f}(T)/t_c$, is not large, less than a factor of about 5.6 in the entire temperature range where $\tau_{QENS,s}(T)$ was available for the 10, 20, and 30% PEO blends. From these two points, the conclusion is justified that the CM provides an explanation of the insensitivity of segmental dynamics of PEO to blend composition at short times observed in deuteron NMR experiments by Ediger and co-workers,[4,6] and in QENS by Sakai et al.[43,44,57]

Explanations from the Lodge−McLeish Model and by Others. The surprisingly fast PEO segmental dynamics and their weak composition dependence in blends of d4PEO/PMMA found by deuterium ^{2}H NMR at high frequencies by Lutz et al.[4] are anomalous in comparison to other miscible polymer blends. The unusual dynamic properties found poses a problem for some early models of polymer blends based on intermolecular composition fluctuations.[37,65,66] They offer no predictions concerning the component dynamics when the concentration becomes sufficiently dilute that each chain is surrounded by repeat units of the other component (notwithstanding chain connectivity, of course). At low concentration of d4PEO dilution such as the 3% d4PEO blend, intermolecular composition fluctuations are absent, and the models cannot explain the data.

The failure of the models of polymer blends based on intermolecular composition fluctuations to address the unusual properties of the fast PEO segmental dynamics led Lutz et al. to provide an explanation by themselves. They were faced by the fact that the ratio, $\tau_{seg,slow}/\tau_{seg,fast}$, of the segmental relaxation times of the slow PMMA component to the fast PEO component segmental at the DSC T_g for the blend is 10^{11} to 10^{12} times. Thus, the PMMA segments adjacent to the PEO are immobile on the time scale of PEO motion. Lutz et al.[4] proposed the lack of side groups on PEO is the key to the PEO chains to locally relax despite the PMMA chains are effectively frozen. The absence of a side group may allow nearly complete conformational relaxation of PEO without requiring any conformational rearrangement of nearby PMMA segments. In this way, Lutz et al. explained both the large difference between segmental dynamics of the two components and the weak composition dependence of PEO segmental dynamics. From this, they further explain why the PEO segmental relaxation has a weaker temperature dependence than that of the terminal relaxation time of PEO chains found by Colby[33] and Zawada et al.[34] because the latter involves rearrangement of the entire PEO chain in the blends.

High-frequency ^{13}C NMR relaxation measurements performed by He et al.[2] on miscible polymer blends of polybutadiene (PB) with poly(vinyl ethylene) (PVE) also found the unusual fast PB segmental dynamics with weak dependence on composition similar in behavior to the PEO segmental dynamics in blends of d4PEO/PMMA. PB has no side group like PEO, and its fast segmental dynamics was explained by weak coupling between PB and dPVE chains in the same way as proposed for PEO and PMMA. The CM explanation given in subsection (A) for the d4PEO/PMMA blends applies to the PB/PVE blends as well because the measurements were performed at high frequencies.

The Lodge−McLeish (LM) model was proposed to interpret and predict the component dynamics in miscible polymer mixtures.[38] It considers the self-concentration effect, i.e., the enhanced local concentration due to the connectivity of the polymer chain) by assuming that the segmental relaxation process of a given segment in a polymer mixture is affected by the effective local concentration ϕ_{eff} in a surrounding region with a length scale of the Kuhn segment l_K. This ϕ_{eff} is calculated from the bulk concentration ϕ and the self-concentration ϕ_{self} by the equation,

$$\phi_{eff} = \phi_{self} + (1 - \phi_{self})\phi \quad (3)$$

In eq 3, ϕ_{self} is determined from the volume fraction occupied by one Kuhn length of the polymer inside a volume $V = l_k^3$ and is given by

$$\phi_{self} = C_\infty M_0/\kappa\rho N_{AV} V \quad (4)$$

In eq 4 C_∞ is the characteristic ratio, M_0 is the repeat unit molar mass, κ is the number of backbone bonds per repeat unit, ρ is the density, and N_{AV} is Avogadro's number. This model provides qualitatively correct predictions of dynamics in miscible polymer blends in the high-temperature regime well above the blend T_g.

The predictions of the LM model[38] were used by Lutz et al.[4] to fit the fast PEO segmental dynamics in blends of d4PEO/

https://doi.org/10.1021/acs.jpcb.4c03520
J. Phys. Chem. B 2024, 128, 10709−10726

PMMA by varying the self-concentration ϕ_{self} utilizing the VFT parameters for pure d4PEO and assuming a Fox relationship for the blend T_g. The results of the best LM model fit of the blend data from Lutz et al. are reproduced in Figure 3. The value of ϕ_{self} for the best fits is 0.57. The LM model provides reasonable fits to the data, and the value of ϕ_{self} predicted by their eq 4 is 0.15. Similarly, large ϕ_{self} values of 0.55 and 0.64 were deduced from the variation of T_g with blend composition for PEO with PMMA and PVAc respectively by Gaikwad et al.[67] The best LM fit of the fast segmental relaxation times for PEO in the blend with PVAc from ^{2}H NMR at 15.6 and 76.7 MHz was obtained by Zhao et al.[6] with ϕ_{self} = 0.30, which is still larger than the value of 0.15 predicted by eq 4 of the model.

The same discrepancy between ϕ_{self} for the best fits and ϕ_{self} predicted by the LM model was found in the study of He et al.[2] for the fast segmental relaxation of polybutadiene (PB) in blends with poly(vinyl ethylene) (PVE). The values of ϕ_{self} from fitting are 0.71 and 0.59 for *cis*-PB and *trans*-PB are different from the prediction of ϕ_{self} = 0.29 calculated from eq 4 of the LM model.

One reason was suggested by He et al.[2] for this disagreement between ϕ_{self} predicted by the eq 4 of the LM model and ϕ_{self} for the best fits of the fast PB segmental dynamics in blends with PVE. They pointed out that the model implicitly assumes that the dynamics of the two components are strongly coupled with each other. This assumption is at odds with the weak coupling of PB to PVE due to PB having no side group invoked[2] to explain the fast PB segmental dynamics observed, like PEO in blends with PMMA[4] or with PVAc discussed before.

TWO DISTINCT CALORIMETRIC GLASS TRANSITIONS IN BLENDS

There is another reason for the disagreement pointed out later in the paper on miscible blends of polyisoprene (PI) and poly(4-*tert*-butylstyrene) (P4tBS) by Zhao, Ediger, Sun, and Yu.[7] In the blends xPI-(1 − x)P4tBS two distinct calorimetric glass transitions were detected at $T_g^{\alpha 1}$ and $T_g^{\alpha 2}$ in blends with lower x values by Zhao et al.[7] and Arrese-Igor et al.,[68] as well as in the xPEO-(1 − x)PMMA and xPEO-(1 − x)PVAc blends by Mpoukouvalas and Floudas,[39] Silva et al.,[69] Lodge et al.,[51] Leroy et al.,[70] and Urakawa et al.[71] A review of these data is given in ref 72. At temperatures above the higher than T_{g1} of the blend associated with the high T_g component, the faster component is in the equilibrium state, and the LM model is applicable to explain its segmental relaxation. However, below T_{g1}, the matrix is frozen and the glassy environment experienced by the fast component changes the temperature dependence of the segmental relaxation time $\tau_{\alpha 2}$ to become Arrhenius-like. Zhao et al.[7] demonstrated this change in the segmental dynamics of the slow and fast components in a miscible polymer blend schematically in a figure. Thus, at temperatures below T_{g1}, the LM model prediction is no longer applicable. Forcing it to fit the fast component segmental relaxation times above and below T_{g1} results in the discrepancy between ϕ_{self} for the best fits and ϕ_{self} predicted by the LM model as done for PEO in blends with PMMA[4] shown in Figure 3, and also for PB in blends with poly(vinyl ethylene).[2] The change of the PEO (PI) segmental dynamics on crossing T_{g1} in blends with PMMA or PVAc (P4tBS) from equilibrium to nonequilibrium is key to fully understanding the properties of these polymer blends studied by Ediger and co-workers.[2−7] For this reason, the research and advances made in component dynamics of these and other highly asymmetric polymer blends are relevant to the works of Ediger and co-workers considered in this paper and discussed in the following subsections.

***x*PVME-(1 − *x*)PS Blends.** Dynamics of the two components in binary polymer blends of poly(vinyl methyl ether) (PVME, T_g = 250 K) and PS (T_g = 373 K) with large ΔT_g = 123 K were studied by Lorthioir et al.[73] in 2003. In this study, DSC measurements detected two glass transitions in blends with $c_{PVME} \geq 30\%$, but only the upper glass transition temperature $T_g^{\alpha 1}$ = 337 K of the α1-relaxation in the blend with lower c_{PVME} = 20%. Nevertheless, Leroy et al.[70] also in 2003 was able to detect both $T_g^{\alpha 1}$ = 337 K and the lower $T_g^{\alpha 2}$ = 293 K in the blend with c_{PVME} = 20% by the thermally stimulated depolarization current (TSDC) technique shown in Figure 4a. Assuming that $\tau_{\alpha 2}$ at the

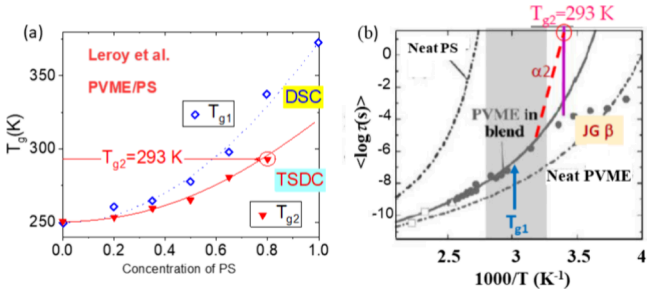

Figure 4. (a) T_g values for the PVME/PS blends as a function of PS concentration obtained from DSC (blue diamonds)[73] and thermally stimulated depolarization current (TSDC) (red triangles).[71] For the blend with 0.8 PS, the values of $T_g^{\alpha 2}$ = 293 K and $T_g^{\alpha 1}$ = 337 K are obtained by TSDC and DSC. (b) Relaxation map of <logτ(s)> for the 20%PVME blend together with the values of $T_g^{\alpha 2}$ and $T_g^{\alpha 1}$ obtained in (a). Also shown are the averaged relaxation times <log$\tau_{diel}(T)$> of the fast relaxation (filled circles) taken from refs 70,73−75, deduced from isothermal dielectric spectra of the fast relaxation. Reproduced with permission from ref 72. Copyright 2021 Elsevier.

TSDC $T_g^{\alpha 2}$ = 293 K is 100 s, shown in Figure 4b is that its temperature dependence below $T_g^{\alpha 1}$ = 337 K is Arrhenius, as suggested by the red line in the figure.

The TSDC $T_g^{\alpha 2}$ = 293 K for c_{PVME} = 20%[71] is a natural extension of the DSC $T_g^{\alpha 2}$ = 280 K for c_{PVME} = 30%. Inexplicably this TSDC $T_g^{\alpha 2}$ = 293 K for c_{PVME} = 20% and the α2 associated with it was not considered by Lorthioir et al.[73] This is likely due to the influence of their own idea at temperatures below T_g of the 20% blend that the PVME is confined by the frozen matrix and the relaxation α' becomes localized and noncooperative. The interpretation was reaffirmed in two reviews,[74,75] and in papers reporting neutron scattering studies.[75,77−79] This conception led them to identify the fast α' relaxation of PVME in the 20% blend as localized and noncooperative resembling a secondary relaxation observed dielectrically either isochronally at 1 Hz at 228 K or isothermally at frequencies $f_{diel}(T)$ from 228 to 328 K (see Figure S2a,c in SI). The corresponding relaxation times $\tau_{diel}(T) = 1/2\pi f_{diel}(T)$ are shown in Figure 4b and also in Figure S2b. Figure 4b is adapted from Figure 9b of the review in 2007 by Colmenero and Arbe,[74] which was republished verbatim as Figure 17b in another review in 2016 by Alegria and Colmenero.[75] The broad shaded area in Figure 4b or Figure 9b in ref 74 and Figure 17b in ref 75 inserted by them clearly indicate they have only a single T_g from DSC for the blend. Other issues and problems of the interpretation given by the authors of refs 74 and 75 are discussed in refs 32 and 72.

It is clear from Figure 4b that there are two PVME-related relaxations below $T_g^{\alpha 1}$ = 337 K. The authors of refs 73−75

https://doi.org/10.1021/acs.jpcb.4c03520
J. Phys. Chem. B 2024, 128, 10709−10726

ignored the one determined by TSDC with $\tau_{\alpha 2}$ = 100 s at $T_g^{\alpha 2}$ = 293 K, which is the truly confined but still cooperative $\alpha 2$ relaxation. On the other hand, the α' relaxation they found from dielectric relaxation has the characteristics of the Johari−Goldstein (JG) β relaxation of PVME in the 20% blend. As pointed out in refs 32 and 72, these characteristics include $\tau_{diel}(T)$ changing temperature dependence from a weak Arrhenius below $T_g^{\alpha 2}$ = 293 K to a stronger one above it and the increase in its dielectric strength with temperature. The activation energy E_a of the $\tau_f(T)$ for the 20%PVME blend in Figure 4b is 7869 K in temperature units, and the ratio, $E_a/T_g^{\alpha 2}$ = 26.9, falls within the bounds of the values for JGβ relaxation in pure glass-formers.[80] All these were observed by Lorthioir et al.[73] and republished in the reviews.[74,75]

***x*PEO-(1 − *x*)PMMA Blends.** The discussion of Figure 4b on the 20% PVME blend with PS shows the presence of three relaxations. The slowest is the $\alpha 1$ relaxation detected by DSC at $T_g^{\alpha 1}$. The intermediate one is the confined but cooperative $\alpha 2$-relaxation detected by TSDC at $T_g^{\alpha 2}$ but not resolved in the dielectric spectra. The fast one is the JGβ relaxation appearing prominently in the dielectric spectra, which was mistaken by Lorthioir et al.[73] and reaffirmed later by their co-authors.[74,75] This mistake should be recognized by others and not repeated in considering the other blends, *x*PEO-(1 − *x*)PMMA and *x*PI-(1 − *x*)PtBS, studied by Ediger and co-workers.[4−7] To ensure this, pertinent data for these two blends are discussed.

The DSC measurements of Floudas and co-workers,[39] Lodge and co-workers,[51] and Silva et al.,[69] detected two glass transitions at $T_g^{\alpha 2}$ and $T_g^{\alpha 1}$. In the relaxation map of Figure 5, the magenta star placed at 100 s is supposed to represent the $\alpha 2$-relaxation time $\tau_{\alpha 2}$ of the PEO component at $1000/T_g^{\alpha 2}$ with $T_g^{\alpha 2}$ = 245 K in the 20% PEO−80% PMMA blend. The $\alpha 2$-relaxation of the PEO component was not resolved in the dielectric studies of Runt and co-workers[41,42,81] because it is obscured by the dielectric loss over a broad frequency range from the JG β relaxation of the PMMA component. However, it was observed in blends of perdeuteriopoly(ethylene oxide) (d4PEO) and PMMA using deuteron NMR over the concentration range from 0.5 to 100% d4PEO with Larmor frequencies ranging from 31 to 76 MHz by Ediger and co-workers discussed before and shown in Figures 1−3. In the inset of Figure 5, in addition to the same symbols and line in the main figure, we show by asterisks the data for PEO in the 25/75 blend from QENS at Q = 1.02 Å^{-1} by Genix et al.[76] (appearing in Figure 6 of ref 78), and the other symbols are other QENS data of Sakai et al.[43] Absent are the dielectric data of $\tau_{\alpha 2}$ over the range $10^{-10} < \tau_{\alpha 2} < 10^2$ s. Although a VFT function can be found to fit the deuteron NMR data and for it to reach $\tau_{\alpha 2}(T_g^{\alpha 2})$ = 100 s at $T_g^{\alpha 2}$ = 245 K from DSC as shown by the pale blue line, the high value of about 140 for the fragility index m is not expected for the confined $\alpha 2$-relaxation in the frozen PMMA matrix. Also, the temperature dependence of confined $\tau_{\alpha 2}(T)$ is Arrhenius-like at temperatures above $T_g^{\alpha 2}$. So the blue line in Figure 5 better represents the Arrhenius T-dependence of $\tau_{\alpha 2}(T)$ in the range of $10^{-10} \ll \tau_{\alpha 2} < 10^2$ s. Dielectric relaxation measurements of the 20% PEO blend with PMMA made by Runt and co-workers observed a secondary relaxation having practically the same relaxation times as in pure PEO, and identifiable as the JG β relaxation of PEO in the blend. Most of its relaxation times, τ_β, were obtained at temperatures lower than the range in Figure 5. Notwithstanding, by showing some values of τ_β at higher temperatures by the magenta line (labeled JG β) in Figure 5, the presence of the three major processes, the $\alpha 1$-relaxation, the confined but cooperative $\alpha 2$-relaxation, and the JG β relaxation, is clear.

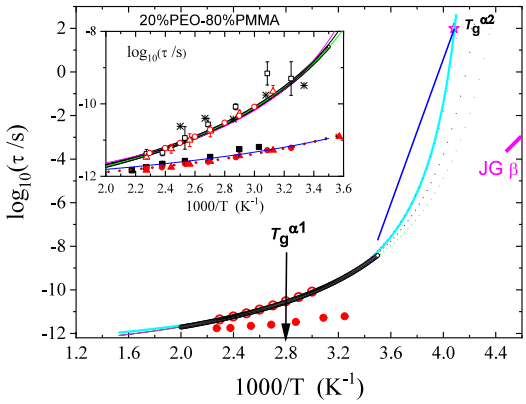

Figure 5. In the main figure, the line defined by open black circles is the fit of ^{2}H NMR data of segmental α-relaxation time of the PEO component from Lutz et al.[4] in 20% PEO−80% PMMA blend. The magenta star is placed at 100 s to represent the $\alpha 2$-relaxation time $\tau_{\alpha 2}$ of the PEO component at $T_g^{\alpha 2}$ = 245 K in the 20% PEO−80% PMMA blend. The closed and open red circles are the fast and slow $\alpha 2$-relaxation times found in QENS experiment of Garcia-Sakai et al. at Q = 1.3 Å^{-1}.[57,58] The vertical black arrow locates the position of $T_g^{\alpha 1}$ = 356 K for the PMMA component in the blend. The pale blue line is the VFT fit of the NMR data of the PEO component in 20% PEO−80% PMMA blend and requires it to reach $\tau_{\alpha 2}(T)$ = 100 s at $T_g^{\alpha 2}$ = 245 K, which is not acceptable because it is out of equilibrium. The blue line is the Arrhenius T-dependence of the confined $\alpha 2$-relaxation suggested to interpolate $\tau_{\alpha 2}(T)$ = 100 s at $T = T_g^{\alpha 2}$ and the deuteron NMR data (open black circles). The short and thick magenta lines represent the relaxation times of the JG β relaxation. In the inset, in addition to the same symbols and line in the main figure, it shows QENS data for PEO in the 25/75 blend from QENS at Q = 1.02 Å^{-1} (asterisks) from Genix et al.[76,78] Also from QENS data at Q = 1.02 Å^{-1} are open black squares indicating the slow relaxation, and the closed black squares the fast relaxation for the PEO component in the 20%PEO-80%PMMA blend. The red closed and open triangles are the same for the 30%PEO-70% PMMA blend. The blue line is the primitive relaxation time of PEO obtained from NMR data of pure PEO. Reproduced with permission from ref 72. Copyright 2021 Elsevier.

SEGMENTAL VERSUS TERMINAL DYNAMICS OF PEO IN PMMA

The deuteron NMR segmental relaxation times $\tau_{\alpha,PEO,x}(T)$ of PEO in blends with PVAc from the work of Ediger and co-workers[6] show a weaker temperature dependence than the terminal dynamics of PEO in the same blends. The effect is anomalous because in pure PEO the T-dependence of segmental relaxation and terminal relaxation at high temperatures are nearly the same.[6] In contrast, measured by dielectric spectroscopy at frequencies below 10^6 Hz, the segmental relaxation time $\tau_{\alpha 2}$ of PI in the blend 35%PI/65%PtBS has either a stronger than or about the same temperature dependence as the normal mode of PI (see Figure 9b in ref 82 and also Figures 4 and 5 in ref 59). Even pure PI has the temperature dependence of its segmental relaxation time τ_α stronger than that of the normal mode,[83,84] and this is consistent with the CM equations for the two processes having different frequency dispersions or coupling parameters n.[31,32,66,67] This normal behavior in pure polymers was first discovered by Plazek.[85−87]

The anomalous behavior is more spectacular in *x*PEO/(1 − *x*)PMMA blends when comparing the deuteron NMR

https://doi.org/10.1021/acs.jpcb.4c03520
J. Phys. Chem. B 2024, 128, 10709−10726

$\tau_{\alpha,\mathrm{PEO},x}(T)$ with the tracer diffusion factor D and terminal relaxation time τ_{terminal} of unentangled PEO with low molecular weight in the xPEO/(1 − x)PMMA blends for x = 0.3% by Haley and Lodge,[50] and for x = 1, 10, and 20% PEO by Zeroni et al.[56] Shown in Figure 6, the monomeric friction factor $\zeta_{\mathrm{PEO},x}(T)$

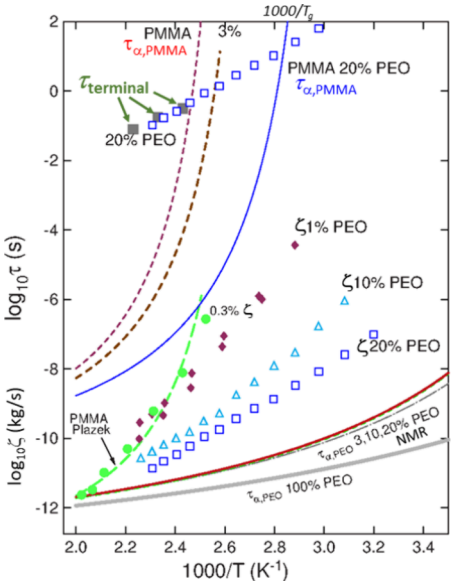

Figure 6. Temperature dependences of the PEO segmental α-relaxation times in (1) the PEO homopolymer (thick gray line at bottom), and (2) in the blends with x = 3, 10, and 20% of PEO with PMMA (lines above the PEO homopolymer). The dielectric segmental relaxation times of pure PMMA (magenta dashed line), and the VFT dependence of segmental relaxation time of the PMMA component in blends with 3% (brown line) and 20% PEO (blue line) from Lutz et al.[4] The symbols are monomeric friction factors $\zeta_{\mathrm{PEO},x}(T)$ of PEO chains in blends of x = 0.3 (green circles), 1 (magenta diamonds), 10 (pale blue triangles) and 20% (blue squares) PEO with PMMA from Haley and Lodge.[50] The exception are the gray closed squares, which are the terminal relaxation times τ_{terminal} of PEO in blend of 20% PEO with PMMA from Colby,[33] and the temperature dependence is similar to $\zeta_{\mathrm{PEO},x}(T)$ in the blend with the same x = 20. This is demonstrated by shifting the data of $\zeta_{\mathrm{PEO},x}(T)$ upward (open blue squares) to compare them with τ_{terminal}. The green dashed line represents the temperature dependence of the shift factors of the Rouse modes of pure PMMA in the glass−rubber transition dispersion zone.[88] It is shifted (green dashed line) to show the same temperature dependence as that of $\zeta_{\mathrm{PEO},x}(T)$ for x = 0.3 (green closed circles). Reproduced with permission from ref 32. Copyright 2023 Elsevier.

for the PEO tracers[50,56] determined by diffusion and rheology was found to be a much stronger function of temperature than the deuteron NMR $\tau_{\alpha,\mathrm{PEO},x}(T)$ measured at high frequencies by Lutz et al.[4] Represented by different symbols, $\zeta_{\mathrm{PEO},x}(T)$ of the x = 0.3, 1, 10, and 20% PEO tracer each changes by five-four orders of magnitude. On the other hand, over the same temperature range, the segmental relaxation times $\tau_{\alpha,\mathrm{PEO},x}(T)$ of PEO in 0.5, 3, 6, 10, 20, and 30% PEO blends (represented by lines) changes either little or by less than 1 order of magnitude. Moreover, while $\zeta_{\mathrm{PEO},x}(T)$ decreases rapidly with increasing concentration x of PEO, by contrast, $\tau_{\alpha,\mathrm{PEO},x}(T)$ from deuteron NMR hardly decreases with x. The direct proportionality relationship $\zeta_{\mathrm{PEO},x}(T) \propto \tau_{\alpha,\mathrm{PEO},x}(T)$ expected by Lodge and co-workers[50,56] is violated. Their findings led to the following conclusions. The global dynamics of a PEO tracer in a PMMA matrix cannot be simply related to the PEO segmental dynamics. PEO tracer friction factors are many orders of magnitude larger than what is predicted from the segmental dynamics. Additionally, the global dynamics are a much stronger function of temperature than the segmental dynamics (see Figure 6). Also shown in Figure 6 are the terminal relaxation times τ_{terminal} of 20% PEO in blends with PMMA obtained rheologically by Colby (gray closed squares on the upper left corner).[33] The temperature dependence of τ_{terminal} is the same as $\zeta_{\mathrm{PEO},x}(T)$ for the same x = 20% from diffusion. This is demonstrated in the figure by shifting $\zeta_{\mathrm{PEO},x}(T)$ (blue squares) upward to overlap with the τ_{terminal}.

CM Explanation. The spectacular difference between $\zeta_{\mathrm{PEO},x}(T)$ and $\tau_{\alpha,\mathrm{PEO},x}(T)$ found by Lodge and co-workers[50,56] shows once more the impact of the deuteron NMR works by Ediger et al.,[4,6] which poses difficulty for any theory, but are consistent with the CM predictions of the deuteron NMR $\tau_{\alpha,\mathrm{PEO},x}(T)$ from eq 2.[45,48,54] The crux of the explanation of why τ_{terminal} and $\zeta_{\mathrm{PEO},x}(T)$ having much stronger temperature dependence than the deuteron $\tau_{\alpha,\mathrm{PEO},x}(T)$ is still the unusual PEO component dynamics probed by deuteron NMR at high frequencies and high temperatures. The experimental condition forces the primitive relaxation times $\tau_0(T)$ of the CM to approach crossover time $t_c \sim 2$ ps. By virtue of the CM eq 2, $\tau_{\alpha,\mathrm{PEO},x}(T)$ becomes insensitive to changes in the composition and local environment of the blends. Furthermore, the diffusion of a tracer PEO chain in the PMMA matrix involves global motion which is different from the local segmental relaxation in nature and length-scale of the dynamics. The tracer PEO chain cannot diffuse without some motion of the matrix PMMA chains. Thus, the temperature dependence of the diffusion coefficient or the monomeric friction coefficient of the PEO tracer chain is determined by the matrix PMMA chains. The length scale of the PMMA motion necessary for the PEO tracer to diffuse depends on the molecular weight of the PEO tracer. For the low molecular weight unentangled PEO tracer used by Haley and Lodge,[50] the shift factors of the PEO tracer diffusion coefficient may be closer to that of the Rouse dynamics of the PMMA matrix given by Plazek and co-workers. It could be accidental, but nevertheless remarkable, that this Rouse dynamics shift factor of PMMA changes by about the same orders of magnitude as the PEO tracer diffusion coefficient over the same temperature range as shown in Figure 6.

The many orders of magnitude stronger temperature dependence of the global chain dynamics than that of the segmental dynamics found for PEO in PEO/PMMA blends are not found for either the polyisoprene (PI) component in blends with poly(vinylethylene) (PVE)[3] or the polybutadiene (PB) component in blends with PVE.[2] It is not found in homopolymers such as atatic polypropylene.[9] The explanation from the CM is that τ_0 of PI or PB in Figure 1 is much longer than t_c.[45] When substituted into eq 2, the much larger values of $\tau_0(T)/t_c$ entail the much larger value and stronger temperature dependence of $\tau_{\alpha,\mathrm{PI},x}(T)$ or $\tau_{\alpha,\mathrm{PB},x}(T)$ in the blends of PI or PB with PVE shown before in Figure 1.

Other Explanation. Lutz et al.[4] gave an explanation of the stronger T-dependence of PEO chain diffusion and terminal relaxation time than the deuteron NMR segmental α-relaxation time of PEO in blends with PMMA or PVAc. The absence of a side group of PEO enables conformational relaxation of PEO without requiring any conformational rearrangement of nearby PMMA segments. In contrast, terminal relaxation requires that the end-to-end vector of the chain be rearranged. As far as the

https://doi.org/10.1021/acs.jpcb.4c03520
J. Phys. Chem. B 2024, 128, 10709−10726

best of our knowledge, no other explanation has been offered in the literature.

BREAKDOWN OF STOKES–EINSTEIN AND DEBYE–STOKES–EINSTEIN RELATIONS

Ediger and co-workers made many contributions in observing the breakdown of the Stokes–Einstein (SE) and the Debye–Stokes–Einstein (DSE) relations by different experimental techniques.[10−20] These experiments involving measurements of the self-diffusion coefficient D were achieved for three different molecular glass-formers, indomethacin,[10] *tris*-naphthylbenzene,[18] and *ortho*-terphenyl[19] over a range of temperatures down to T_g. In contrast to $D \propto \eta^{-1}$ given by the SE relation between D and viscosity η and to $D \propto \tau_\alpha^{-1}$ by the DSE relation, the fractional power relation of $D \propto \eta^{-\lambda}$ and $D \propto \tau_\alpha^{-\lambda}$ with $\lambda < 1$ were observed. The values of λ are 0.76, 0.77, and 0.80 for indomethacin, *tris*-naphthylbenzene and *ortho*-terpenyl, respectively. Consequently, the measured D exceeds the value predicted by the SE relation by about 2 orders of magnitude at T_g. These valuable experimental data over a wide range of temperatures are remarkable achievements of Ediger and co-workers and have an impact on theoretical explanations as discussed below.

Explanation by Spatially Heterogeneous Dynamics. Using novel NMR techniques applied to the α-relaxation in poly(vinyl acetate) above T_g, Schmidt-Rohr, and Spiess[89] discovered that the process associated with the nonexponential correlation function is heterogeneous with a distribution of correlation times. On the time scale of the average correlation time, the process becomes homogeneous. This spatially heterogeneous dynamics or dynamic heterogeneity in supercooled liquids had been confirmed in other systems including colloidal particles using confocal microscopy by Weeks and Weitz[90] and by simulations of Lennard–Jones liquids by Donati et al.[91] The relaxation times differ from one region of space to another, and near T_g, these times can vary greatly from location to location, even close by.

The existence of spatially heterogeneous dynamics was used by Ediger[20] to explain the breakdown of Debye–Stokes–Einstein and the Stokes–Einstein relations between diffusion and viscosity or relaxation time, based on earlier works by others.[92−95] It assumes regions of differing dynamics give rise to the Kohlrausch relaxation function of the structural α-relaxation in ensemble averaging. The decoupling between self-diffusion and rotation occurs because D and τ_c are averages over different moments of the distribution of relaxation times, with $D \propto <1/\tau>$ emphasizing fast dynamics, while $\tau_c \propto <\tau>$ is determined predominantly by the slowest molecules.

Support of the spatially heterogeneous interpretation of the breakdown came from the empirical correlation found between the enhanced translation given by the product, $D\tau_c$, at T_g with the Kohlrausch nonexponentiality parameter β_K at T_g for probes in five glass-formers: *o*-terphenyl, *tris*(naphthyl)benzene, polystyrene, polysulfone, and polyisobutylene (see Figure 11 in ref 20). The correlation found is expected if both enhanced translation and nonexponential rotation are due to spatially heterogeneous dynamics. Notwithstanding, the correlation is also consistent with an alternative explanation of the difference between translational diffusion and rotational relaxation in supercooled liquids by the CM,[96] where more experimental data were considered (see Figures 1 and 2 of ref 96).

In order for the spatially heterogeneous explanation to be consistent with the observed monotonic increases of products $D\eta$ and $D\tau_c$ as the temperature is lowered toward T_g, the breadth of the relaxation time distribution has to increase (or the Kohlrausch exponent β_K has to decrease) correspondingly. However, the dielectric spectra of *tris*-naphthylbenzene (TNB) are characterized by a temperature-independent width (e.g., β_K is constant and is equal to 0.50) from T_g = 345 up to $T_B \approx 417$ K.[97] Photon correlation spectroscopic[98] and NMR[99] measurements all indicate a temperature-independent distribution of relaxation times. Thus, the data of TNB are not consistent with the explanation based on spatial heterogeneities. The same was found in *ortho*-terphenyl by Richert[100] and sucrose benzoate by Rajian et al.[101] These evidence from experiments as well as from simulations[102,103] led to the conclusion in refs 19 and 104 that spatial and dynamic heterogeneity of the structural relaxation cannot explain the breakdown of the Debye–Stokes–Einstein and Stokes–Einstein relations without modifications.

CM Explanation. An alternative explanation[96] of the breakdown of the SE and DSE relations was proposed by the CM based on its eq 1, now generalized to become $\tau_\mu = [t_c^{-n_\mu}\tau_{0\mu}]^{1/(1-n_\mu)}$. This form is applicable for different dynamic variables μ related to diffusion, rotation, and viscosity, and they have different coupling parameters n_μ. Applying these CM equations to the various μ, the one having a larger n_μ will bestow a longer and stronger temperature dependence for its relaxation time τ_μ, as demonstrated in ref 49. This is because the primitive relaxation times of all observables $\tau_{0\mu}$ should have comparable values and the same temperature dependence. This CM explanation applies straightforwardly when n_μ is independent of temperature from T_B down to T_g as found in experiments[97,100,101] and demonstrated in ref 49. The demonstration was performed with n_D = 0.37 for diffusion assumed to be smaller than n_d = 0.50 for rotation known from dielectric measurement, and the results are presented in Figure S3 in the Supporting Information. The CM was able in ref 96 to explain the empirical correlation found between the enhanced translation given by the product, $D\tau_c$, at T_g with the Kohlrausch nonexponentiality parameter β at T_g for probes in many different glass-formers.

Support of the CM explanation of the breakdown of the SE and DSE relations without assuming the value of n_D[32,49,105] came from molecular dynamics simulation of an equimolar mixture of interacting Gay-Berne ellipsoids of revolution and Lennard-Jones spheres along an isochore at a series of temperatures down to the deeply supercooled state by Chakrabarti and Bagchi.[106] Also known are the other coupling parameters n_1 and n_2 of the first- and second-rank single particle orientational time correlation functions, $C_1(t)$ and $C_2(t)$. The CM explanation is quantitative, and the predictions compare well with the simulation data. It is worthwhile to present the results in more detail in Section S1 and Figure S4 of SI. Also in ref 96, it is explicitly stated that the dynamics in the CM is heterogeneous and ref 107 was cited in support. However, the review[20] considered the CM in ref 96 as a homogeneous explanation for experimental observations of enhanced translational diffusion. In order to rectify this misunderstanding, I quote from ref 96 the statements: "The CM interpretation of enhanced translation diffusion does not contradict outright the proposed explanations that are based on the spatially heterogeneous dynamic of the molecules and, particularly, dynamic heterogeneity. As was mentioned before, the molecular dynamics in the coupling model are consistent with dynamic

https://doi.org/10.1021/acs.jpcb.4c03520
J. Phys. Chem. B 2024, 128, 10709−10726

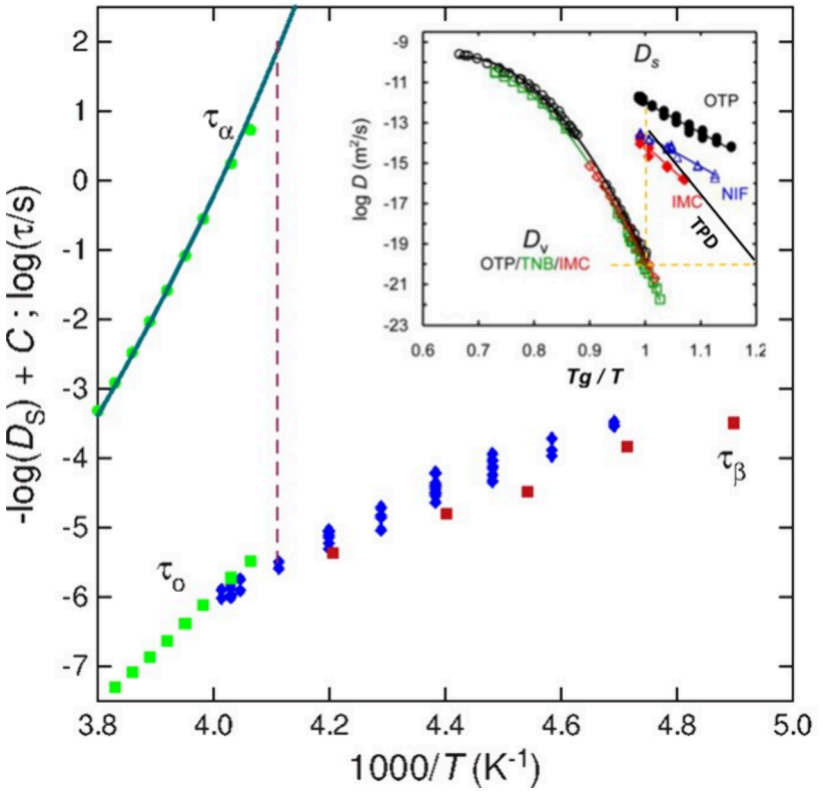

Figure 7. Green closed circles and squares are the α-relaxation times $\tau_\alpha(T)$, and the primitive relaxation times $\tau_0(T)$ (calculated), and the red closed squares are the JG β-relaxation times $\tau_\beta(T)$) of bulk OTP. The blue closed diamonds represent $-\log D_S(T) + C$ with $C = -17.35$ and the original data of $D_S(T)$ are from ref 108. The inset showing $D_S(T)$ and $D_V(T)$ is reproduced from ref 108 (ACS Publishing). Added is the line that is a fit of the $D_S(T)$of the OG of TPD by the Arrhenius dependence. Figure by, *Phys. Chem. Chem. Phys.*, 2017, 19, 29905/CC BY 3.0. Reproduced from *Phys. Chem. Chem. Phys.*, 2017, 19, 29905, ref 116. Available under a CC-BY 3.0 license. Copyright 2017 Ngai, K. L.; Paluch, M.; Rodriguez-Tinoco, C.

heterogeneity. In fact, one earlier formulation of the CM based on the "Dining Philosophers Problem" in computer science[107] gave a vivid demonstration that cooperative relaxation has to be dynamically heterogeneous and is the source of the non-exponential KWW function (eq 5). This paper[107] was published in 1990, 1 year before the seminal experimental work of Schmidt-Rohr and Spiess,[89] which proves that the dynamic is heterogeneous. Thus, the results of the CM based on the KWW functions include the dynamic heterogeneous nature of the KWW function."

■ ENHANCED SURFACE MOBILITY

The studies of enhanced mobility of molecules of glass-forming liquids on a free surface than in the bulk by Ediger, Lian Yu, and co-workers[21−28,108,109] and also by others[110−118] are important not only for basic research on the dynamics of the structural α-relaxation but also in utilizing the effect to produce glasses with exceptionally high density and stability by physical vapor deposition.[119−126] Surface diffusion coefficients $D_S(T)$ of several molecular glass-formers including indomethacin (IMC),[21] *tris*-naphthyl benzene,[22] ethylbenzene,[24] and *ortho*-terphenyl (OTP)[110] were measured at temperatures slightly above and mostly below the bulk glass transition temperature T_g using the method of surface-grating decay. The surface diffusion coefficients $D_S(T)$ are found to be many orders of magnitude larger than the bulk diffusion coefficients $D_V(T)$ at the same temperature. The different sizes of the increases from $D_V(T)$ to $D_S(T)$ for different materials found by the experiments are an additional challenge for any theory to explain.

Explanation by the Random First Order Transition (RFOT) Theory. The RFOT theory[127] of the structural glass dynamics by Lubchenko and Wolynes has explained quantitatively many bulk glass phenomena. The structural relaxation time of the bulk $\tau_{bulk} = \tau_0 \exp(F_{bulk}/k_BT)$ is determined by the free energy barrier for reconfiguration events in the bulk. Stevenson and Wolynes[128] argued that the free energy barrier at the surface is reduced from F_{bulk} by a factor of two. Very near to the surface, the relaxation time is related very simply to the bulk value by the relation,

$$\tau_{surf} = (\tau_0 \tau_{bulk})^{1/2} \tag{5}$$

Apparently, this prediction of τ_{surf} by eq 5 at the bulk glass transition temperature T_g where $\tau_{bulk}$is a long time, say 10^3 s, can vary for different glass-formers depending on the value τ_0. However, quantitative testing of the prediction with experimental data of many different glass-formers from Ediger, Lian Yu, and co-workers has not been carried out so far. Due to the large variations in the ratio τ_{surf}/τ_{bulk} at the bulk glass transition temperature T_g found experimentally, the prediction $\tau_{surf}/\tau_{bulk} = (\tau_0/\tau_{bulk})^{1/2}$ at the bulk T_g from RFOT by eq 5 is not able to explain them.

Explanation by the ECNL Theory of Mirigian and Schweizer. Based on their quantitative, force-level theory of relaxation in bulk supercooled liquids, the elastically collective nonlinear Langevin equation (ECNLE) theory,[129−131] Mirigian and Schweizer (MS) extended it to free-standing films and surfaces to predict the spatial mobility gradient.[132] Near the surface both local caging constraints and spatially long-range

https://doi.org/10.1021/acs.jpcb.4c03520
J. Phys. Chem. B 2024, 128, 10709−10726

collective elastic distortion are reduced, resulting in mobility gradient calculated using molecular parameters representative of van der Waals liquids. MS applied the theory in ref 133 to near-surface translational diffusion and compared the predictions to the experiments of Ediger, Yu, and co-workers. They defined two different diffusion constants, $D_{surface,A} \approx d^2/6<\tau_{\alpha,bulk}>_w$ or $D_{surface,B} \approx (d^2/6)<1/\tau_{\alpha,bulk}>_w$, in averaging the near-surface layer dynamics to different penetration depths, w, and compared with $D_{bulk} \approx d^2/6<\tau_{\alpha,bulk}>$. Here, d is the diameter of hard spheres in the theory. By using $D_{surface,A} \approx d^2/6<\tau_{\alpha,bulk}>_w$, MS found diffusion is 4 or 8 decades faster than D_{bulk} at the bulk T_g for $w = d$ and $0.5d$, respectively. These values are consistent with the 6 to 8 decades of enhancement obtained from surface diffusion experiments by Ediger, Yu, and co-workers[21−28,108,109] for molecular glass-formers. If $D_{surface,B} \approx (d^2/6)<1/\tau_{\alpha,bulk}>_w$ is used, the enhancement is even larger since the more rapidly relaxing regions strongly dominate the transport. The enhancement at the bulk T_g is ∼10 decades, which is much larger than that found experimentally. A quantitative comparison of the prediction of either $D_{surface,A}$ or $D_{surface,B}$ with a particular glass-former has been made so far.

CM Explanation. Free of neighboring molecules and totally free of space to explore on one side, molecules diffusing on the surface are devoid of intermolecular coupling. Thus, for the CM at the surface, the coupling parameter n_S in eq 1 can become zero or nearly zero, and the surface diffusion time $\tau_S(T)$ is the same or nearly the same as $\tau_0(T)$. The CM predicts the surface diffusion coefficient, $D_S(T)$, which is given by $D_S(T) = d^2/4\tau_0(T)$. By contrast, in the bulk, the coupling parameter n is nonzero and the bulk diffusion coefficient $D_V(T)$ is given by $D_V(T) = d^2/6\tau_\alpha(T)$ with $\tau_\alpha(T)$ determined by the CM equation,

$$\tau_\alpha = [t_c^{-n_\alpha}\tau_0]^{1/(1-n_\alpha)} \tag{6}$$

It follows from eq 6 that

$$\frac{D_S(T)}{D_V(T)} = \frac{\tau_\alpha(T)}{\tau_0(T)} = [\frac{\tau_\alpha(T)}{t_c}]^{n_\alpha} \tag{7}$$

Eq 7 makes it possible for the CM to predict the ratio $D_S(T)/D_V(T)$ quantitatively from the known values of $\tau_\alpha(T)$, n_α, and t_c of the bulk material. Examples of the applications of the CM are given as follows.

OTP and Indomethacin. The cases of OTP[108] and IMC[21] are presented in Figures 7 and S5 in the SI, respectively. The size of the enhancement of D_S over D_V depends on the glass-former, as shown by nearly 2 orders of magnitude more in the case of OTP than in IMC, which is correlated with the larger coupling parameter $n_\alpha = 0.50$ for OTP[116] than $n_\alpha = 0.41$ for IMC.[110] By using this value of n_α together with the choice of $\tau_\alpha(T_g) = 10^3$ s to define T_g, the CM eq 6, gives $\tau_\alpha(T_g)/\tau_0(T_g) = 10^{7.5}$, which is in order of magnitude agreement with the experimentally observed surface diffusion enhancement $D_s(T_g)/D_v(T_g)$ in OTP[25,116] (see Figure 7) and IMC[21,110] (see Figure S5). The result $D_s(T_g)/D_v(T_g) = 10^{7.5}$ is obtained by using the dielectric or viscosity $n_\alpha = 0.50$ for the OTP, and not n_D for diffusion. The value of n_D is unknown but expected to be smaller than n_α, and thus the actually predicted enhancement $D_s(T_g)/D_v(T_g)$ is less than $10^{7.5}$, and smaller than the experimental value by possibly one to two decades. The discrepancy may be removed if the difference in thermodynamic factor at the surface compared to the bulk if taken into account.

One can find in both figures the approximate agreement between the relaxation times $\tau_\beta(T)$ of the Johari−Goldstein (JG) β relaxation and the calculated $\tau_0(T)$, which is another prediction of the CM,[31,32,134−136]

$$\tau_\beta(T) \approx \tau_0(T) \tag{8}$$

This relation in eq 8 has been used to distinguish the special class of intermolecular secondary relaxations (JGβ) having strong connections to the α relaxation from the trivial intramolecular ones. It has been verified in many glass-formers of different types[31,32] since the first paper[134] in 1998, and is justified by both the primitive relaxation and the JG β relaxation are noncooperative or nonfully cooperative precursors of the structural α-relaxation and have similar properties. The properties of the JGβ relaxation are also linked to those of α relaxation[31,32,134−136] such as pressure dependence and TV^γ dependence in thermodynamic scaling.[137]

Above T_g, the shift of $\tau_0(T)$ with the temperature in Figure 7 is parallel to that of $D_s(T)$. Below T_g, the temperature dependence of $\tau_\beta(T)$ from the experiment is also approximately the same as $D_s(T)$. These experimental results are consistent with the additional prediction from the CM that the temperature dependence of $D_s(T)$ is similar to that of $\tau_\beta(T) \approx \tau_0(T)$. This is a unique opportunity to test and verify the CM prediction of bulk $\tau_\alpha(T)$ will become its $\tau_\beta(T, P) \approx \tau_0(T, P) = (t_c)^n\tau_\alpha^{1-n}$, not only above T_g but also below T_g when cooperativity is completely removed on the free surface or when nanoconfined. The high-quality surface diffusion data obtained by Mark Ediger, Lian Yu, and co-workers are much appreciated by the author for using them in applying the CM.

Ethylcyclohexane (ECH). The JGβ relaxation in this molecular glass-former (ECH) is located close to the α-relaxation and the two relaxations overlap.[138−140] Consequently the frequency dispersion of the α-relaxation at temperatures above T_g is artificially broadened and the actual stretch exponent β_K of the Kohlrausch correlation function or coupling parameter $n = (1 - \beta_K)$ cannot be determined from the dielectric and mechanical spectra.[117] Nevertheless the actual value of $n \approx 0.30$ was deduced from dielectric data of the structurally close-related cyanocyclohexane (CNCH). The calculated value of primitive relaxation time $\tau_0(T)$ at T_g is consistent with experimental JGβ relaxation times $\tau_\beta(T)$ near T_g from dielectric spectroscopy. Below T_g, the dielectric $\tau_\beta(T)$ is also compatible with the JGβ relaxation time $\tau_{ac}(T)$ from adiabatic calorimetry[117,141] (see Figure 8). Surface diffusion measurements performed on ECH, as reported in ref 23 provide the surface diffusion times $\tau_{surface}(T)$. Unfortunately, the incorrect n value deduced from the fit of the artificially broadened dielectric α-loss peak in refs 138−140 was used in ref 23 to test the CM prediction of $\tau_{surface}(T) \approx \tau_0(T) \approx \tau_\beta(T)$. Naturally, the CM prediction is violated by the use of the inappropriately inflated value of n, as done and reported in ref 23. This misunderstanding was rectified in ref 117 by using the suitable and justified value of n near 0.30, and approximate agreement of $\tau_{surface}(T)$ with the calculated $\tau_0(T)$, the experimental $\tau_\beta(T)$ and $\tau_{ac}(T)$ is restored. This is shown in Figure 8. More details can be found in ref 117.

Metallic Glass, $Pd_{40}Cu_{30}Ni_{10}P_{20}$. The surface diffusion coefficient $D_s(T)$ of the metallic glass, $Pd_{40}Cu_{30}Ni_{10}P_{20}$ was measured by the method of surface-grating decay.[111] $D_s(T_g)$ was found to be more than 8 orders of magnitude larger than the bulk diffusion coefficient $D_v(T_g)$. The CM was applied in a similar manner as in the case of OTP and IMC to predict the size of the surface diffusion found in $Pd_{40}Cu_{30}Ni_{10}P_{20}$ (Pd40).[112] The experimental data of bulk and surface diffusion are shown in Figure S6 in the SI. The CM predicts the enhancement of

https://doi.org/10.1021/acs.jpcb.4c03520
J. Phys. Chem. B 2024, 128, 10709−10726

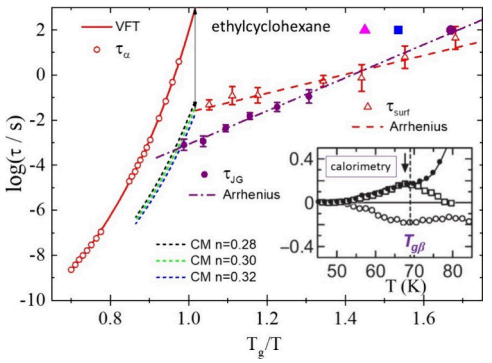

Figure 8. Relaxation times τ_α (open circles) and $\tau_{surface}$ (open triangles) of ethylcyclohexane (ECH) plotted against T_g/T with T_g = 100 K. The τ_α data were taken from ref 139. and the $\tau_{surface}$ data come from ref 23. The solid line is the VFT fit of the temperature dependence of τ_α. The dashed line is the fit to $\tau_{surface}$ by the Arrhenius dependence. The three dotted lines represent the calculated primitive relaxation times τ_0 with n = 0.32, 0.30, and 0.28, and the differences between them are small. In addition, τ_{JG} (purple circles) taken from ref 139. is plotted against T_g/T along with its Arrhenius fit (purple dash-dotted line). The large filled magenta triangle and purple circle respectively represent τ_{JG} ($T_{g\beta}$ = 69 K) ≈ $\tau_0(T_{g\beta}$ = 69 K) = 100 s at $T_g/T_{g\beta}$ = 1.45 and $\tau_{JG}(T_{g\beta}$ = 60 K) ≈ $\tau_0(T_{g\beta}$ = 60 K) = 100 s at $T_g/T_{g\beta}$ = 1.67. The blue square is similar adiabatic calorimetry result for *sec*-butylcyclohexane with T_g = 129 K and $T_{g\beta}$ = 84 K. The inset show the heat-release/-absorption rates for bulk ECH within glassy state from adiabatic calorimetry measurements in ref 141. The arrow locates 69 K. The solid and open circles represent respectively the data for the samples prepared by rapid (−5 K min^{-1}) and slow (−20 mK min^{-1}) precooling; with their smooth behaviors being portrayed by the respective solid lines. Open squares in some of the insets represent the data obtained in a sample prepared by rapid precooling with intermediate annealing at 80 K. Reproduced with permission from ref 117. Copyright 2021 Elsevier.

mobility at the surface compared to the bulk, $D_s(T_g)/D_v(T_g)$, which can be estimated by $\tau_\alpha(T_g)$ $/\tau_0(T_g)$. The value of the coupling parameter n of $Pd_{40}Cu_{30}Ni_{10}P_{20}$ is 0.46, obtained from the fit to the shear loss modulus data by the Fourier transform of the Kohlrausch function with stretch exponent $\beta_K \equiv (1-n)$ = 0.54. The value of t_c of metallic glasses is 0.2 ps shorter than 2 ps of van der Waals glass-formers due to stronger metallic interactions.[32] The primitive frequencies, logf_0, calculated by the CM equation with $t_c \approx 0.2$ ps, n = 0.46 and $\tau_\alpha(T_g) = 10^3$ s, gives $\log[\tau_\alpha(T_g)/\tau_0(T_g)]$ = 7.2 for Pd40 in Figure S6, which is about 1 order of magnitude smaller than the experimental value of $\log[D_v(T_g)/D_s(T_g)]$.

SAME SURFACE DIFFUSION $D_S(T)$ IN SG, OG, AND NANOTHIN FILM

Fakhraai and co-workers[113−115] investigated the effect of variations in bulk dynamics on the surface diffusion of the molecular glass, *N*,*N*′-bis(3-methylphenyl)-*N*,*N*′-diphenylbenzidine (TPD) with its ordinary T_g = 330 K. Using the tobacco mosaic virus as a probe particle, they measured $D_S(T)$ on glasses of the same composition but with large differences in bulk relaxation dynamics, and in the glass transition temperatures. The glasses include ordinary glass (OG) obtained by liquid quenching, annealed glass after physical aging at 0.9T_g for a week, ultrastable glass (SG) fabricated by physical vapor deposition at various substrate temperatures, and 12 to 30 nm thin films of TPD glass. The fictive temperature T_f is reduced in aged glass and much reduced in the SG. The onset temperature for the transformation from the stable glass to the supercooled liquid, T_{on}, is significantly higher than *the* T_g of the OG. These changes imply many orders of magnitude increase in the structural α-relaxation time τ_α. However, despite the large difference in τ_α of SG, OG, and annealed OG, and nanometer-thin films of TPD, the surface diffusion coefficients $D_S(T)$ of these glasses measured turn out to be nearly identical at two temperatures below the T_g of bulk OG. Their data of $D_S(T)$ for OG are compared with τ_α of bulk TPD from dielectric measurements[27,116] as shown in Figure 9, and $D_S(T)$ for the

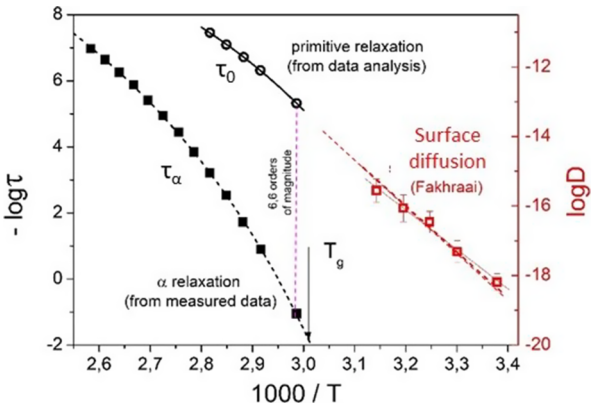

Figure 9. A new plot of the surface diffusion coefficient, D_S, data of ordinary glass (OG) of TPD digitized from the figure in ref 113 against 1000/T (open squares, left axis). Data is compared with bulk relaxation times τ_α (closed squares, left axis) from dielectric relaxation measurements from ref 27. The primitive relaxation times τ_0 are calculated by the CM equation with β_K value determined from dielectric spectra.[116] The relative shift in the data sets to enable them to be compared in the same plot is based on the empirical rule that the bulk diffusion coefficient at T_g is approximately 10^{-20} m^2 s^{-1}, and τ_α is approximately 100 s.[115] Error bars of surface diffusion coefficients were obtained from two repeating trials by Zhang et al., digitized and entered into this new figure.[113]

nanometer-thin films in Figure 10 (Left panel), and $D_S(T)$ for the SG together with OG and aged glass in Figure 10 (Right panel). As emphasized by Zhang and Fakhraai[114]: "The bulk fictive temperatures of these glasses span over 35 K, indicating 13 to 20 orders of magnitude changes in bulk relaxation times. However, the surface diffusion coefficients on these glasses are measured to be identical at two temperatures below the bulk glass transition temperature T_g. These results suggest that surface diffusion has no dependence on the bulk relaxation dynamics when measured below T_g."

The dielectric data[27] were fitted by the Kohlrausch function and the value of $(1-n)$ at temperatures above T_g is 0.5. The $\tau_0(T)$ calculated by the CM eq 1 from the bulk $\tau_\alpha(T)$ with this value of n and shown in the two figures seem to be a continuation of the Arrhenius dependence of the surface diffusion times below T_g obtained from $D_S(T)$ measurements. Good correspondence is another verification of surface diffusion, and $D_S(T)$ is determined by $\tau_0(T)$.

CM Explanation. The remarkable findings by Fakhraai and co-workers had been given an explanation based on the CM.[116] The surface diffusion in all cases involves the removal of intermolecular coupling or cooperativity in relaxation and diffusion of molecules at the surface, resulting in the surface relaxation time $\tau_S(T)$ being the same as the primitive/JGβ relaxation times, $\tau_0(T) \approx \tau_\beta(T)$,[32,134−136] of the CM, and orders of magnitude shorter than the bulk α-relaxation time $\tau_\alpha(T)$. The

https://doi.org/10.1021/acs.jpcb.4c03520
J. Phys. Chem. B 2024, 128, 10709−10726

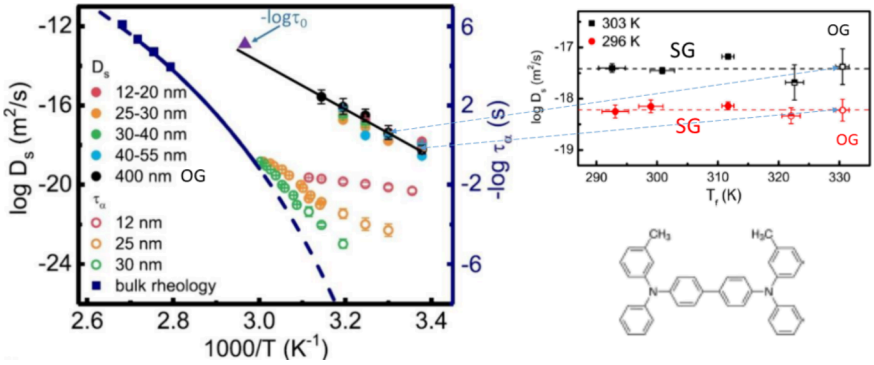

Figure 10. (Left) Surface diffusion coefficients D_S measured on TPD films with thicknesses ranging from 12 to 400 nm (colored solid circles) are plotted along with average bulk relaxation times, τ_α, measured by bulk viscosity (navy blue squares), and dielectric relaxation measurements (solid navy blue line) as a function of $1/T$. The average relaxation times in ultrathin films of 12−30 nm are also plotted for comparison (colored open circles). Added is the primitive relaxation time calculated by the CM equation ref 116 with β_K value obtained from fits of the dielectric spectra from ref 27. Reproduced from ref 115. Copyright 2017 Proc. Natl. Acad. Sci. U. S. A. (Right) Surface diffusion coefficients on stable glasses (SG) (filled), aged glass (half filled), and liquid-quenched glasses (OG) (open) measured at 303 (black) and 296 K (red), plotted versus fictive temperature. The horizontal dashed lines are the average D_s at each temperature showing D_S of SG, OG, and aged glass are all the same. The two dashed lines connect the same D_s data of OG at 303 and 296 K in the two figures. Reproduced with permission from ref 114. Copyright 2017 American Institute of Physics.

enhanced surface diffusion is given by $D_S(T) = d^2/6\tau_S(T) = d^2/6\tau_0(T)$ where d is the size of the molecule. The crux of the explanation of the approximate invariance of $D_S(T)$ in SG, OG with and without physical aging, and nanometer-thin films of TPD is the corresponding approximate invariance of $\tau_0(T) \approx \tau_\beta(T)$, despite the huge differences in $\tau_\alpha(T)$ and the different values of $n(T)$ of the α-dynamics and the changes in thermodynamic conditions. No matter how thin the OG film is, how long the OG is aged, and how OG is transformed to SG by vapor deposition, the $\tau_0(T)$ remains the same, and hence also $D_S(T)$ remains the same. The surface diffusion data of Fakhraai and co-workers[113−115] are highly appreciated by the author in enabling him to test the CM predictions critically.

Explanation by Others. The fact that the surface diffusion coefficient $D_s(T)$ is unchanged in SG, OG, and nanothin films of TPD as found by Fakhraai and co-workers[113−115] is challenging for any theory on surface diffusion to explain. However, other theories[128,132] of surface diffusion have not addressed the experimental data of SG, OG, and nanothin films of TPD, and the CM explanation[116] is the only one published in the literature so far.

JOHARI−GOLDSTEIN β RELAXATION IN ULTRASTABLE GLASSES

Another example of important experimental data from Ediger and co-workers given here is their study of the JGβ relaxation of the SG in toluene prepared by physical vapor deposition, and compare it with that of the OG.[25] They found that 70% of the JGβ relaxation intensity in OG is suppressed in SG, indicating the drastic change in thermodynamic conditions that would require ~3500 years of annealing of the OG to obtain similarly suppressed dynamics. The experimental data of $\tau_\beta(T)$ of a toluene SG deposited at a substrate temperature 98 K (=0.84T_g) from Yu et al.[25] are reproduced in Figure 11, where $\tau_\beta(T)$ and $\tau_\alpha(T)$ of the toluene OG are from dielectric and NMR measurements. Yu et al.[25] found that $\tau_\beta(T)$ of the SG is longer than the OG by about one decade at the same temperature, and the T-dependence of both is Arrhenius with nearly the same activation energies of E_β = 27 ± 3 and 25 ± 2 kJ/mol, respectively.

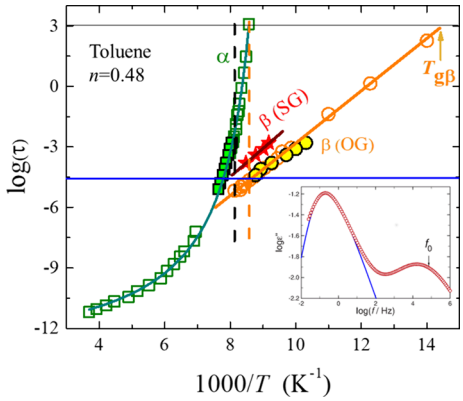

Figure 11. Main figure is reproduced from Yu et al.[25] with permission from APS. It shows logarithmic relaxation times of α and β processes of ordinary glass (open symbols), and the relaxation times for the vapor-deposited samples (solid symbols) vs reciprocal temperature. Added are the two vertical lines located at $1000/T_g$ and $1000/T_{on}$. Inset: the dielectric loss spectrum of toluene, the fit by the Fourier transform of the Kohlrausch function yielding the value of β_K, and the calculated value of the primitive frequency f_0 are in agreement with f_β of the JGβ. Figure from ref 23 and reused with permission from APS. Adapted with permission from ref 25. Copyright 2015 American Physical Society.

Other features in Figure 11 are added to facilitate the CM explanation in ref 118 to be given in the next section. The onset temperature T_{on} of 123 K for the transformation from the SG to the supercooled liquid was determined before by Ahrenberg et al.,[24] and the corresponding $1000/T_{on}$ is located by the vertical black broken line. The other vertical broken line is at $1000/T_g$ with T_g = 117 K. The Arrhenius T-dependence of $\tau_\beta(T)$ in the SG is extrapolated to higher temperatures to intersect $1000/T_{on}$. The intersection determines $\tau_\beta(T_{on}) = 10^{-4.31}$ s for the SG, while a similar operation determines $\tau_\beta(T_g) = 10^{-4.57}$ s for the OG.

The CM relation (8), $\tau_0(T) \approx \tau_\beta(T)$, is verified in toluene above T_g as shown by an example in the inset of Figure 11 from the dielectric loss spectrum at 119 K with f_α = 0.2 Hz from ref 142 and the Kohlrausch fit with exponent $(1 - n) = 0.52$. The calculated primitive frequency $f_0 = (1/2\pi\tau_0)$ is about half a decade higher than $f_\beta = (1/2\pi\tau_\beta)$, verifying the relation (8) and

https://doi.org/10.1021/acs.jpcb.4c03520
J. Phys. Chem. B 2024, 128, 10709−10726

demonstrating the observed secondary relaxation in toluene is of the JGβ kind.[134−136]

The same properties of the JGβ relaxation in SG and OG of toluene had been found in two other molecular glass-formers, etoricoxib, and telmisartan by Rodriguez-Tinoco et al.,[143] and shown in Figure S7 in the SI. Kasting et al.[144] investigated the barely resolved relaxation in SG and OG of methyl-*m*-toluate, which has been confirmed to be the JGβ relaxation by applying pressure.[145,146] Like toluene, the JGβ relaxation of etoricoxib, telmisartan, and methyl-*m*-toluate becomes *slower* in the SG than OG.[143] All these are truly the intermolecular JGβ relaxation with strong and inseparable connections to the α relaxation and satisfying the criteria of the classification.[134−136] The CM explanation was provided in ref 118.

Studied also in ref 143 are the secondary relaxations in SG and OG glasses of β-D-maltose octa-acetate, carvedilol, and celecoxib. Known before from their properties in the supercooled liquid state, these secondary relaxations do not belong to the class of JGβ relaxations and have no connection to the α relaxation in properties. Unsurprisingly, they behave differently from JGβ relaxation in β-D-maltose octa-acetate, carvedilol, and celecoxib by becoming *faster* in the SG than in the OG.[143]

It is worthwhile to note that we[118,143] distinguished the JGβ relaxation from the intramolecular non-JGβ relaxation[134,135,145] when considering the changes from OG to SG. On the other hand, Kasting et al.[144] did not do so and considered all of them together as well as in ref 126.

CM Explanation. An explanation was given by the CM based on two general properties established from the studies of glasses and liquids at elevated pressures and applied to SG. The increase in the density of the glasses formed under high pressure can be even larger than that in SG, yet the change of τ_β is small.[118] Derived from the Coupling Model, there are two properties. One is the approximate invariance of the ratio $\tau_\alpha(T_{on})/\tau_\beta(T_{on})$ to density change at constant $\tau_\alpha(T_{on})$, and the other is the same ρ^γ/T-dependence of τ_β in SG and OG where ρ is the density and γ is a material constant.[137] Details of the CM explanation are not repeated here but can be found in ref 118. It was referenced in the review by Berthier and Ediger.[126] This explanation is related to that given before for understanding the same surface diffusion coefficient being found in SG and OG with and without physical aging and ultrathin films of a molecular glass-former.

Glass with a density higher than USG can be realized by applying pressure P much higher than ambient pressure $P_0 = 0.1$ MPa. If the changes in the magnitude and activation energy of τ_β in USG compared to OG are general, they should be observed by elevating pressure from P_0 to P.[118] The answer is positive from the results of studies at elevated pressures.[147,148] An example is the isobaric data of DGEBA (diglycidyl ether of bisphenol A, M_w = 380 g/mol, also known as EPON 828). Shown in Figure S8 are the α-relaxation times τ_α and JG β-relaxation times τ_β at ambient pressure P_0 of 0.1 MPa and at P = 400 MPa. Defining glass transition temperatures by $\tau_\alpha = 100$ s, we have $T_g = 252.8$ K at P_0 and $T_{gP} = 306.7$ K at P = 400 MPa. The increase of 54 K is significantly larger than that expected for USG. The value of $\tau_\beta(T_g,P_0)$ is about the same as that of $\tau_\beta(T_{gP},P)$. The activation energy is $E_\beta = 52.2$ kJ/mol at ambient pressure, and it is about the same as the value at P = 400 MPa. Thus, the relation of τ_β at high pressure to ambient pressure is the same as that of USG to OG. The ratio $\tau_\beta(T,P)/\tau_\beta(T,P_0)$ ≈100 is larger, and this is consistent with the larger density increase by elevated pressure. The frequency dispersion of the α relaxation or the value of n_α in eq 6 is invariant to changes of T and P for EPON 828[147,148] and in general for other van der Waals glass-formers.[32] For the same $n_\alpha = 0.48$ and $\tau_\alpha = 100$ s at ($T_g = 252.8$ K, P_0) and ($T_{gP} = 306.7$ K, P = 400 MPa) in Figure S8, the CM eqs 6 and 8 predicts $\tau_\beta(T_g,P_0)$ is about the same as $\tau_\beta(T_{gP},P)$. This is clearly verified in Figure S8, and it supports the CM explanation for the JGβ relaxation in SG compared to OG mentioned in the previous paragraph.

Explanation by Others. Although the studies of the change of the secondary relaxation from OG to SG are widely publicized in publications,[25,118,126,143,144] no explanation of the experimental findings has been given by others. This is perhaps unsurprising since the secondary relaxations in neither the potential energy landscape models of Johari and Goldstein,[149] and Goldstein,[150] nor the random first-order transition theory of Stevenson and Wolynes[151] can be applied in the present forms to this problem. Apparently, the only explanation of the SG and OG data[25,143,144] is that given by the CM.[118]

Notwithstanding, Berthier and Ediger (BE)[126] were concerned with CM explanation by the statement "⋯ *the time scale τ_β measured experimentally decreases with the aging time for a number of systems* (their refs 64 and 37) *whereas the structural relaxation presumably increases instead, suggesting that care is needed to relate τ_β to τ_α in an unambiguous manner.*"

The systems BE referred to in their ref 37 (corresponding to ref 143 herein) are β-D-maltose octa-acetate, carvedilol, and celecoxib. As mentioned before and explained already in refs 118 and 143, the secondary relaxations in these three glass-formers are intramolecular and non-JGβ relaxations. Unlike the true JGβ relaxations of toluene, etoricoxib, and telmisartan, they have no connection to and correlation with the α relaxation in properties, and thus their relaxation times can become faster in SG than in OG. Thus, this concern of BE is not real.

The glass-former BE referred to in their ref 64 is the aging study of the polymer 1,2-polybutadiene or PVE by Casalini and Roland.[152] On aging PVE, its JGβ relaxation time is nearly unchanged or decreases slightly by less than a factor 2 with increasing aging time t_e.[152] An explanation of this finding was given before in Section 2.3.2.20, starting on page 405 in ref 31 Aging in PVE and some other glass-formers can cause an increase in the coupling parameter n in eq 6. With $n(t_e)$ an increasing function of t_e, the CM relation now takes the form,

$$\tau_\beta(t_e) \approx \tau_0(t_e) = [\tau_\alpha(t_e)/t_c]^{1-n(t_e)}t_c \quad (9)$$

On the right-hand side of this eq 9, some slight increase of $n(t_e)$ with t_e can compensate for the increase of $\tau_\alpha(t_e)$ to maintain $\tau_\beta(t_e)$ relatively unchanged or even increasing slightly. Such increase of $n(t_e)$ with t_e was found on aging of a very rapidly quenched polystyrene by creep compliance measurements shown in Figure 80 of ref 31, and reproduced here as Figure S9 in the SI. A sizeable increase of n on aging with a small change of the fast or primitive relaxation time was observed in colloidal suspensions of hard spheres and Laponite presented in Section 2.2.5.4 in ref 31, with the heading "Correlation Between n and Aging Time". In the aging experiment of PVE,[148] Casalini and Roland used the CM eq 1 together with $\tau_\beta(T) \approx \tau_0(T)$ at temperatures below T_g and found the calculated $\tau_\alpha(T)$ are in good agreement with that from the experiment.

JGβ Glass Transition Temperature $T_{g\beta}$. JGβ relaxation strongly coupled to the α relaxation can be seen from the primitive relaxation time τ_0 calculated from τ_α via eq 6, which is indeed approximately equal to τ_β from experiments, i.e. eq

https://doi.org/10.1021/acs.jpcb.4c03520
J. Phys. Chem. B 2024, 128, 10709−10726

8.[32,134] Eq 6 also requires $\tau_0 \approx \tau_\beta$ to have a dependence on entropy, enthalpy, and specific or free volume as τ_α does, although the dependences are different due to the dependence of the latter is obtained from the former by raising it to the power of $1/(1-n)$, as shown in eq 6. The same argument leads to $\tau_0 \approx \tau_\beta$ and τ_α being different functions of the same thermodynamics scaling variable TV^γ which is also found in experiments.[137] On decreasing temperature and at some temperature, $T_{g\beta}$, τ_0, or τ_β becomes too long for the structure to be maintained, and the JGβ glass transition occurs. Like the primary glass transition, it is detectable by calorimetry via enthalpy, and positron annihilation lifetime spectroscopy (PALS) via specific volume, albeit it is weaker and hence more difficult due to lesser sensitivity.[32] For an example from ethylcyclohexane (ECH), see the inset of Figure 8.

As discussed in the previous subsections, enhanced surface diffusion coefficient D_S is critical for the formation of ultrastable glasses. Enhancement is caused by the total removal of cooperativity at the surface, and in the CM explanation the surface diffusion time is related to the primitive relaxation time $\tau_0(T)$ or the JG β-relaxation time $\tau_\beta(T) \approx \tau_0(T)$ from eq 8. If the temperature of the substrate for the formation of the SG by vapor deposition is lowered, $\tau_\beta(T)$ becomes longer and the enhancement of surface diffusion is reduced. One can expect the lowest substrate temperatures possible for the formation of SGs to be reached at the secondary glass transition temperature $T_{g\beta}$, where $\tau_\beta(T_{g\beta})$ reaches 10^3 s. The expansive research by Ediger and co-workers on the formation of SGs provides rich information on the dependence of the stability of glasses on substrate temperature. Their data enable a test of the expected behavior related to $T_{g\beta}$ and $\tau_\beta(T_{g\beta})$ from the CM. This expectation was verified in ref 153 by the dependence of the stability of vapor-deposited molecular glasses on substrate temperature from experiments. The molecular SGs considered include toluene,[24] ethylbenzene,[24] ethyl cyclohexane,[23] methyl-*m*-toluate,[29] celecoxib,[123] *ortho*-terphenyl,[122] and *cis*-decalin.[109] The demonstrations are given in Figures S10 and S11 in the SI.

DISCUSSION AND CONCLUSIONS

The research areas of the dynamics and thermodynamics of complex materials cover many different classes of materials involving different processes. In the past many decades and continuing to the present times, a myriad of experiments and simulations have been carried out, yielding a vast collection of data and results. Of particular interest to theorists are those results that lead to the discovery of general properties. Concomitantly a variety of theories and models have been proposed with success to explain the general properties. However, as is usually the case, the foundations, assumptions, and key factors of the different theories proposed are very different. The dilemma is that there is no way to tell which theory offers the correct explanation. One possible resolution of the dilemma is for someone to perform experiments with new results that can critically test all theories proposed to find out which is the correct one. The important tasks for experimentalists were carried out by Mark Ediger and his collaborators, as well as by Fakhraai and co-workers, in several research areas of relaxation and diffusion in complex materials made known in this tribute to Mark Ediger's illustrious career.

The Coupling Model (CM) has benefitted from their experimental studies and findings by its theoretical predictions from eqs 6 and 8 being rigorously tested and found consistent with the experimental data presented in this paper. The same situation applies to much more experimental data from other workers in different research areas, as demonstrated in the recent comprehensive review.[32] Naturally, the question asked is why the CM equations are so prolific and widely applicable. The answer comes from the classical chaos (i.e., nonlinear Hamiltonian mechanics) arising from the anharmonic interaction in materials, which is the fundamental physics in the CM. Applied to relaxation and diffusion, theory and computations of simplified models[31] found classical chaos engenders cooperative many-body relaxation and diffusion with the stretched exponential time correlation function of Kohlrausch, $\exp-(t/\tau_\alpha)^{1-n}$. Notwithstanding, the effect of classical chaos starts only after a characteristic time, t_c determined by the strength of the intermolecular potential. Before t_c, the correlation function is a linear exponential function, $\exp-(t/\tau_0)$, of one-body relaxation and diffusion. This predicted crossover of the correlation function from $\exp-(t/\tau_0)$ to $\exp-(t/\tau_\alpha)^{1-n}$ at t_c was confirmed by experiments and simulations in various materials.[31,32] The continuity of the two pieces of the correlation at t_c leads to eq 6. Derived from a physical law or principle, the CM equation is generally applicable to explain many different experimental data in various materials. In all these explanations by eq 6, the nonexponentiality of the many-body cooperative relaxation represented by the coupling parameter n in the CM plays a crucial role. A shortcoming of the CM eq 6 is not providing information on the motion of the particles or molecules spatially and the evolution with time, i.e., the heterogeneous nature of the dynamics found experimentally. Nevertheless, generated by the chaos of the many-body-interacting particles or molecules, the processes exemplified by the Kohlrausch correlation function $\exp-(t/\tau_\alpha)^{1-n}$ cannot be homogeneous. Despite spatially heterogeneous dynamics being the rule, it has not been used much to explain other experimental findings[31,32] including most of those considered in this paper. It was used to explain qualitatively the breakdown of the Debye–Stokes–Einstein relation but it failed so far. Heterogeneous dynamic and Kohlrausch stretched exponential are parallel consequences of the many-body cooperative relaxation and diffusion in materials governed by anharmonic interactions. It is not easy to quantify by either experiment or theory the degree of heterogeneity and use it to correlate or explain dynamic and thermodynamic properties. On the other hand, the degree of nonexponentiality or the coupling parameter n of the CM can be routinely obtained by experiment and simulations, and used in the CM eq 6 to correlate and explain a voluminous amount of experimental data.[31,32] In contrast, other theories did not do the same.

ASSOCIATED CONTENT

Supporting Information

The Supporting Information is available free of charge at https://pubs.acs.org/doi/10.1021/acs.jpcb.4c03520.

Self-intermediate scattering function for hPEO in dPMMA; dielectric spectra and relaxation map of PVME/PS blends; temperature dependence of dielectric and diffusion times of TNB; breakdown of Debye–Stokes–Einstein relation; data from a simulation of translational and rotational diffusion; temperature dependence of various relaxation times of bulk and surface diffusion of indomethacin and $Pd_{40}Cu_{30}Ni_{10}P_{20}$; Arrhenius plot of τ_β in stable glass and an ordinary glass of toluene, etoricoxib, and telmisartan; creep compliance of polystyrene; Relaxation dynamics and stability of vapor-

https://doi.org/10.1021/acs.jpcb.4c03520
J. Phys. Chem. B 2024, 128, 10709−10726

deposited simple molecule glasses, toluene, ethylbenzene, ethyl cyclohexane, methyl-*m*-toluate, celecoxib, *ortho*-terphenyl, and *cis*-decalin (PDF)

AUTHOR INFORMATION

Corresponding Author

K. L. Ngai − *CNR-IPCF, Institute for Chemical and Physical Processes, I-56127 Pisa, Italy*; orcid.org/0000-0003-0599-4094; Email: kiangai@yahoo.com, ngaikia@gmail.com

Complete contact information is available at: https://pubs.acs.org/10.1021/acs.jpcb.4c03520

Notes

The author declares no competing financial interest.

Biography

K.L.N. received his PhD in Condensed Matter Physics in 1969 from the University of Chicago. From 1969 to 1971, he was a member of the research staff at Lincoln Laboratory of Massachusetts Institute of Technology. Starting from 1971 he performed research at Naval Research Laboratory, Washington, DC until his retirement in 2010. Since 2010, he has continued doing research in association with CNR-IPCF in Pisa, Italy, and Yansan University, People's Republic of China. He invented the Coupling Model for relaxation and diffusion in complex systems in 1979 which predicted universal properties. In the past 45 years, he applied the predictions to various processes in different classes of materials to verify the universal properties and apparently has succeeded in this endeavor, https://doi.org/10.1016/j.pmatsci.2023.101130.

ACKNOWLEDGMENTS

The author thanks CNR-IPCF for appointment as Ricercatore Associato con incarico di collaborazione Senior.

REFERENCES

(1) Min, B.; Qiu, X.; Ediger, M. D.; Pitsikalis, M.; Hadjichristidis, N. Component dynamics in polyisoprene/polyvinylethylene blends well above T_g. *Macromolecules* **2001**, *34*, 4466−4475.

(2) He, Y.; Lutz, T. R.; Ediger, M. D. Comparison of the Composition and Temperature Dependences of Segmental and Terminal Dynamics in Polybutadiene/Poly(vinyl ethylene) Blends. *Macromolecules* **2004**, *37*, 9889.

(3) Haley, J. C.; Lodge, T. P.; He, Y.; Ediger, M. D.; von Meerwall, E. D.; Mijovic, J. Composition and temperature dependence of terminal and segmental dynamics in polyisoprene/poly(vinylethylene) blends. *Macromolecules* **2003**, *36*, 6142−6151.

(4) Lutz, T. R.; He, Y.; Ediger, M. D.; Cao, H.; Lin, G.; Jones, A. A. Rapid poly(ethylene oxide) segmental dynamics in blends with poly(methyl methacrylate). *Macromolecules* **2003**, *36*, 1724−1730.

(5) Lutz, T. R.; He, Y.; Ediger, M. D. Segmental Dynamics of Dilute Polystyrene Chains in Miscible Blends and Solutions. *Macromolecules* **2005**, *38*, 9826−9835.

(6) Zhao, J.; Zhang, L.; Ediger, M. D. Poly(ethylene oxide) Dynamics in Blends with Poly(vinyl acetate): Comparison of Segmental and Terminal Dynamics. *Macromolecules* **2008**, *41*, 8030−8037.

(7) Zhao, J.; Ediger, M. D.; Sun, Y.; Yu, L. Two DSC Glass Transitions in Miscible Blends of Polyisoprene/Poly(4-tert-butylstyrene). *Macromolecules* **2009**, *42*, 6777−6783.

(8) Inoue, T.; Cicerone, M. T.; Ediger, M. D. Molecular motions and viscoelasticity of amorphous polymers near Tg. *Macromolecules* **1995**, *28*, 3425.

(9) Roland, C. M.; Ngai, K. L.; Santangelo, P. G.; Qiu, X. H.; Ediger, M. D.; Plazek, D. J. Temperature dependence of segmental and terminal relaxation in atactic polypropylene melts. *Macromolecules* **2001**, *34*, 6159−6160.

(10) Swallen, S. F.; Ediger, M. D. Self-diffusion of the amorphous pharmaceutical indomethacin near T_g. *Soft Matter* **2011**, *7*, 10339.

(11) Cicerone, M. T.; Blackburn, F. R.; Ediger, M. D. Anomalous diffusion of probe molecules in polystyrene: evidence for spatially heterogeneous segmental dynamics. *Macromolecules* **1995**, *28*, 8224.

(12) Cicerone, M. T.; Ediger, M. D. Enhanced translation of probe molecules in supercooled *o*-terphenyl: Signature of spatially heterogeneous dynamics? *J. Chem. Phys.* **1996**, *104*, 7210.

(13) Blackburn, F. R.; Wang, C.-Y.; Ediger, M. D. Translational and rotational motion of probes in supercooled 1, 3, 5-tris (naphthyl) benzene. *J. Phys. Chem.* **1996**, *100*, 18249.

(14) Swallen, S. F.; Traynor, K.; McMahon, R. J.; Ediger, M. D.; Mates, T. E. Self-diffusion of Supercooled Tris-naphthalbenzene. *J. Phys. Chem. B* **2009**, *113*, 4600.

(15) Bainbridge, D.; Ediger, M. D. Translational diffusion of rubrene and tetracene in polyisobutylene. *Rheol. Acta* **1997**, *36*, 209.

(16) Cicerone, M. T.; Wagner, P. A.; Ediger, M. D. Translational diffusion on heterogeneous lattices: a model for dynamics in glass forming materials. *J. Phys. Chem. B* **1997**, *101*, 8727−8734.

(17) Ediger, M. D. Can density or entropy fluctuations explain enhanced translational diffusion in glass-forming liquids? *J. Non-Cryst. Solids* **1998**, *235*−*237*, 10−18.

(18) Swallen, S. F.; Bonvallet, P. A.; McMahon, R. J.; Ediger, M. D. Self-diffusion of tris-naphthylbenzene near the glass transition temperature. *Phys. Rev. Lett.* **2003**, *90*, No. 015901.

(19) Mapes, M. K.; Swallen, S. F.; Ediger, M. D. Self-Diffusion of Supercooled o-Terphenyl near the Glass Transition Temperature. *J. Phys. Chem. B* **2006**, *110*, 507−511.

(20) Ediger, M. D. Spatially heterogeneous dynamics in supercooled liquids. *Annu. Rev. Phys. Chem.* **2000**, *51*, 99−128.

(21) Zhu, L.; Brian, C. W.; Swallen, S. F.; Straus, P. T.; Ediger, M. D.; Yu, L. Surface Self-Diffusion of an Organic Glass. *Phys. Rev. Lett.* **2011**, *106*, No. 256103.

(22) Ruan, S.; Zhang, W.; Sun, Y.; Ediger, M. D.; Yu, L. Surface diffusion and surface crystal growth of tris-naphthyl benzene glasses. *J. Chem. Phys.* **2016**, *145*, No. 064503.

(23) Tylinski, M.; Beasley, M. S.; Chua, Y. Z.; Schick, C.; Ediger, M. D. Limited surface mobility inhibits stable glass formation for 2-ethyl-1-hexanol. *J. Chem. Phys.* **2017**, *146*, 203317.

(24) Ahrenberg, M.; Chua, Y. Z.; Whitaker, K. R.; Huth, H.; Ediger, M. D.; Schick, C. In situ investigation of vapor deposited glasses of toluene and ethylbenzene via alternating current chip-nanocalorimetry. *J. Chem. Phys.* **2013**, *138*, No. 024501.

(25) Yu, H. B.; Tylinski, M.; Guiseppi-Elie, A.; Ediger, M. D.; Richert, R. Suppression of β Relaxation in Vapor-Deposited Ultrastable Glasses. *Phys. Rev. Lett.* **2015**, *115*, No. 185501.

(26) Sun, Y.; Zhu, L.; Kearns, K. L.; Ediger, M. D.; Yu, L. Glasses Crystallize Rapidly at Free Surfaces by Growing Crystals Upward. *Proc. Natl. Acad. Sci. U.S.A.* **2011**, *108*, 5990.

(27) Walters, D. M.; Richert, R.; Ediger, M. D. Thermal stability of vapor-deposited stable glasses of an organic semiconductor. *J. Chem. Phys.* **2015**, *142*, 134504.

(28) Ediger, M. D.; Forrest, J. A. Dynamics near free surfaces and the glass transition in thin polymer films: A view to the future. *Macromolecules* **2014**, *47*, 471−478.

(29) Tylinski, M.; Sepúlveda, A.; Walters, D. M.; Chua, Y. Z.; Schick, C.; Ediger, M. D. Vapor-deposited glasses of methyl-m-toluate: How uniform is stable glass transformation? *J. Chem. Phys.* **2015**, *143*, 244509.

(30) Ngai, K. L. Universality of low-frequency fluctuation, dissipation and relaxation properties of condensed matter. I. *Comments Solid State Phys.* **1979**, *9*, 127.

(31) Ngai, K. L. *Relaxation and Diffusion in Complex Systems*; Springer: New York, 2011.

(32) Ngai, K. L. Universal properties of relaxation and diffusion in complex materials: Originating from fundamental physics with rich applications. *Prog. Mater. Sci.* **2023**, *139*, No. 101130.

(33) Colby, R. H. Breakdown of time-temperature superposition in miscible polymer blends. *Polymer* **1989**, *30*, 1275−1278.

(34) Zawada, J. A.; Ylitalo, C. M.; Fuller, G. G.; Colby, R. H.; Long, T. E. Component relaxation dynamics in a miscible polymer blend: poly(ethylene oxide)/poly(methyl methacrylate). *Macromolecules* **1992**, *25*, 2896−2902.
(35) Lartigue, C.; Guillermo, A.; Cohen-Addad, J. P. Proton NMR investigation of the local dynamics of PEO in PEO/PMMA blends. *J. Polym. Sci., Part B: Polym. Phys.* **1997**, *35*, 1095−1105.
(36) Doxastakis, M.; Kitsiou, M.; Fytas, G.; Theodorou, D. N.; Hadjichristidis, N.; Meier, G.; Frick, B. Component segmental mobilities in an athermal polymer blend: quasielastic incoherent neutron scattering versus simulation. *J. Chem. Phys.* **2000**, *112*, 8687−8694.
(37) Kumar, S. K.; Colby, R. H.; Anastasiadis, S. H.; Fytas, G. Concentration fluctuation induced dynamic heterogeneities in polymer blends. *J. Chem. Phys.* **1996**, *105*, 3777−3788.
(38) Lodge, T. P.; McLeish, T. C. B. Self-concentrations and effective glass transition temperatures in polymer blends. *Macromolecules* **2000**, *33*, 5278−5284.
(39) Mpoukouvalas, K.; Floudas, G. Effect of Pressure on the Dynamic Heterogeneity in Miscible Blends of Poly(methyl methacrylate) with Poly(ethylene oxide). *Macromolecules* **2008**, *41*, 1552−1559.
(40) Chung, G. C.; Kornfield, J. A.; Smith, S. D. Component Dynamics Miscible Polymer Blends: A Two-Dimensional Deuteron NMR Investigation. *Macromolecules* **1994**, *27*, 964.
(41) Jin, X.; Zhang, S.; Runt, J. Observation of a fast dielectric relaxation in semi-crystalline poly(ethylene oxide). *Polymer* **2002**, *43*, 6247.
(42) Jin, X.; Zhang, S.; Runt, J. Broadband Dielectric Investigation of Amorphous Poly(methylmethacrylate)/Poly(ethylene oxide) Blends. *Macromolecules* **2004**, *37*, 8110−8115.
(43) García Sakai, V.; Chen, C.; Maranas, J. K.; Chowdhuri, Z. Effect of blending with poly(ethylene oxide) on the dynamics of poly(methyl methacrylate): a quasi-elastic neutron scattering approach. *Macromolecules* **2004**, *37*, 9975−9983.
(44) Sakai, V. G.; Maranas, J. K.; Chowdhuri, Z.; Peral, I.; Copley, J. R. D. Miscible blend dynamics and the length scale of local compositions. *J. Polym. Sci., Part B: Polym. Phys.* **2005**, *43*, 2914−2923.
(45) Ngai, K. L.; Roland, C. M. Unusual Component Dynamics in Poly(ethylene oxide)/Poly(methylmethacrylate) Blends As Probed by Deuterium NMR. *Macromolecules* **2004**, *37*, 2817−2822.
(46) Alegria, A.; Colmenero, J.; Ngai, K. L.; Roland, C. M. Observation of the component dynamics in a miscible polymer blend by dielectric and mechanical spectroscopies. *Macromolecules* **1994**, *27*, 4486−4492.
(47) Ngai, K. L.; Roland, C. M. Component Dynamics in Polyisoprene/Poly(vinylethylene) Blends. *Macromolecules* **1995**, *28*, 4033−4035.
(48) Ngai, K. L.; Roland, C. M. Models for the component dynamics in blends and mixtures. *Rubber Chem. Technol.* **2004**, *77*, 579−590.
(49) Ngai, K. L. Why the glass transition problem remains unsolved? *J. Non-Cryst. Solids* **2007**, *353*, 709−718.
(50) Haley, J. C.; Lodge, T. P. Dynamics of a poly(ethylene oxide) tracer in a poly(methyl methacrylate) matrix: Remarkable decoupling of local and global motions. *J. Chem. Phys.* **2005**, *122*, 234914.
(51) Lodge, T. P.; Wood, E. R.; Haley, J. C. Two calorimetric glass transitions do not necessarily indicate immiscibility: the case of PEO/PMMA. *J. Polym. Sci. B Polym. Phys.* **2006**, *44*, 756−763.
(52) Bedrov, D.; Smith, G. D. A molecular dynamics study of relaxation processes in the dynamical fast component of miscible polymer blends. *Macromolecules* **2005**, *38*, 10314−10319.
(53) Ngai, K. L.; Capaccioli, S.; Roland, C. M. Comment on "A Molecular Dynamics Simulation Study of Relaxation Processes in the Dynamical Fast Component of Miscible Polymer Blends. *Macromolecules* **2006**, *39*, 8543−8543.
(54) Ngai, K. L.; Capaccioli, S. On the relevance of the coupling model to experiments. *J. Phys.: Condens. Matter* **2007**, *19*, No. 205114.
(55) Ngai, K. L. Predicting the changes of relaxation dynamics with various modifications of the chemical and physical structures of glass-formers. *J. Non-Cryst. Solids* **2007**, *353*, 4237−4245.
(56) Zeroni, I.; Ozair, S.; Lodge, T. P. Component terminal dynamics in poly (ethylene oxide)/poly (methyl methacrylate) blends. *Macromolecules* **2008**, *41*, 5033−5041.
(57) García Sakai, V.; Maranas, J. K.; Peral, I.; Copley, J. R. D. Dynamics of PEO in Blends with PMMA: Study of the Effects of Blend Composition via Quasi-Elastic Neutron Scattering. *Macromolecules* **2008**, *41*, 3701−3710.
(58) Maranas, J. K. The effect of environment on local dynamics of macromolecules. *Curr. Opin. Colloid Interface Sci.* **2007**, *12*, 29−42.
(59) Ngai, K. L.; Capaccioli, S. Unified explanation of the anomalous dynamic properties of highly asymmetric polymer blends. *J. Chem. Phys.* **2013**, *138*, No. 054903.
(60) Colmenero, A.; Alegria, A.; Arbe, A.; Frick, B. Correlation between non-Debye behavior and Q behavior of the alpha relaxation in glass-forming polymeric systems. *Phys. Rev. Lett.* **1992**, *69*, 478.
(61) Colmenero, J.; Arbe, A.; Alegría, A. Crossover from Debye to Non-Debye Dynamical Behavior of the α Relaxation Observed by Quasielastic Neutron Scattering in a Glass-Forming Polymer. *Phys. Rev. Lett.* **1993**, *71*, 2603−2606.
(62) Colmenero, J.; Arbe, A.; Coddens, G.; Frick, B.; Mijangos, C.; Reinecke, H. Crossover from Independent to Cooperative Segmental Dynamics in Polymers: Experimental Realization in Poly(Vinyl Chloride). *Phys. Rev. Lett.* **1997**, *78*, 1928.
(63) Zorn, R.; Arbe, A.; Colmenero, J.; Frick, B.; Richter, D.; Buchenau, U. Neutron scattering study of the picosecond dynamics of polybutadiene and polyisoprene. *Phys. Rev. E* **1995**, *52*, 781.
(64) Ngai, K. L. Activation energy and molecular weight dependence of cooperative tracer chains diffusion in highly entangled polymer melts. *J. Polym. Sci.* **2024**, *62*, 2036.
(65) Kamath, S.; Colby, R. H.; Kumar, S. K.; Karatasos, K.; Floudas, G.; Fytas, G.; Roovers, J. E. L. Segmental dynamics of miscible polymer blends: Comparison of the predictions of a concentration fluctuation model to experiment. *J. Chem. Phys.* **1999**, *111*, 6121−6128.
(66) McGrath, K. J.; Roland, C. M. Concentration fluctuations and dynamic heterogeneity in PIP/PVE blends. *J. Non-Cryst. Solids* **1994**, *172*, 891−896.
(67) Gaikwad, A. N.; Wood, E. R.; Ngai, T.; Lodge, T. P. Two Calorimetric Glass Transitions in Miscible Blends Containing Poly-(ethylene oxide). *Macromolecules* **2008**, *41*, 2502−2508.
(68) Arrese-Igor, S.; Alegrıa, A.; Colmenero, J. Comparison of calorimetric and dielectric single component glass transitions in PtBS/PI blends. *Macromolecules* **2010**, *43*, 6406−6413.
(69) Silva, G. G.; Machado, J. C.; Song, M.; Hourston, D. J. Nanoheterogeneities in PEO/PMMA Blends: A Modulated Differential Scanning Calorimetry Approach. *J. Appl. Polym. Sci.* **2000**, *77*, 2034.
(70) Leroy, A.; Alegrıa, A.; Colmenero, J. Quantitative study of chain connectivity inducing effective glass transition temperatures in miscible polymer blends. *Macromolecules* **2002**, *35*, 5587−5590.
(71) Urakawa, O.; Ujii, T.; Adachi, K. Dynamic heterogeneity in a miscible poly(vinylacetate)/poly(ethylene oxide) blend. *J. Non Cryst. Solids* **2006**, *352*, 5042−5049.
(72) Ngai, K. L.; Valenti, S.; Capaccioli, S. Molecular dynamic in binary mixtures and polymer blends with large difference in glass transition temperatures of the two components: A critical review. *J. Non Cryst. Solids* **2021**, *558*, No. 119573.
(73) Lorthioir, C.; Alegría, A.; Colmenero, J. Out of equilibrium dynamics of poly (vinyl methyl ether) segments in miscible poly(styrene)-poly(vinyl methyl ether) blends. *Phys. Rev. E* **2003**, *68*, No. 031805.
(74) Colmenero, J.; Arbe, A. Segmental dynamics in miscible polymer blends: recent results and open questions. *Soft Matter* **2007**, *3*, 1474−1486.
(75) Alegria, A.; Colmenero, J. Dielectric relaxation of polymers: segmental dynamics. *Soft Matter* **2016**, *12*, 7709.
(76) Genix, A. C.; Arbe, A.; Alvarez, F.; Colmenero, J.; Willner, L.; Richter, D. Dynamics of poly(ethylene oxide) in a blend with poly(methyl methacrylate): A quasielastic neutron scattering and

https://doi.org/10.1021/acs.jpcb.4c03520
J. Phys. Chem. B 2024, 128, 10709−10726

molecular dynamics simulations study. *Phys. Rev. E* **2005**, *72*, No. 031808.
(77) Tyagi, M.; Arbe, A.; Colmenero, J.; Frick, B.; Stewart, J. R. Dynamic Confinement Effects in Polymer Blends. A Quasielastic Neutron Scattering Study of the Dynamics of Poly(ethylene oxide) in a Blend with Poly(vinyl acetate). *Macromolecules* **2006**, *39*, 3007.
(78) Genix, A.-C.; Arbe, A.; Arrese-Igor, S.; Colmenero, J.; Richter, D.; Frick, B.; Deen, P. P. Neutron scattering investigation of a diluted blend of poly(ethylene oxide) in polyethersulfone. *J. Chem. Phys.* **2008**, *128*, 184901.
(79) Tyagi, M.; Arbe, A.; Alegria, A.; Colmenero, J.; Frick, B. Dynamic Confinement Effects in Polymer Blends: A Quasielastic Neutron Scattering Study of the Slow Component in Blend Poly(vinyl acetate)/Poly(ethylene oxide). *Macromolecules* **2007**, *40*, 4568.
(80) Ngai, K. L.; Capaccioli, S. Relation between the activation energy of the Johari-Goldstein b relaxation and *Tg* of glass formers. *Phys. Rev. E* **2004**, *69*, No. 031501.
(81) Zhang, S.; Jin, X.; Painter, P. C.; Runt, J. Broad-Band Dielectric Study on Poly(4-vinylphenol)/Poly(ethyl methacrylate) Blends. *Macromolecules* **2002**, *35*, 3636.
(82) Arrese-Igor, S.; Alegría, A.; Moreno, A. J.; Colmenero, J. Effect of Blending on the Chain Dynamics of the "Low-Tg" Component in Nonentangled and Dynamically Asymmetric Polymer Blends. *Macromolecules.* **2011**, *44*, 3611.
(83) Ngai, K. L.; Casalini, R.; Roland, C. M. Volume and Temperature Dependences of the Global and Segmental Dynamics in Polymers: Functional Forms and Implications for the Glass Transition. *Macromolecules* **2005**, *38*, 4363−4370.
(84) Pawlus, S.; Sokolov, A. P.; Paluch, M.; Mierzwa, M. Influence of Pressure on Chain and Segmental Dynamics in Polyisoprene. *Macromolecules* **2010**, *43*, 5845−5850.
(85) Plazek, D. J. 1995 Bingham medal address: Oh, thermorheological simplicity, wherefore art thou? *J. Rheol.* **1996**, *40*, 987.
(86) Ngai, K. L.; Plazek, D. J. Identification of different modes of molecular motion in polymers that cause thermorheological complexity. *J. Rubber Chem. Technol. Rubber Rev.* **1995**, *68*, 376−434.
(87) Ngai, K. L.; Plazek, D. J. A Quantitative Explanation of the Difference in the Temperature Dependences of the Viscoelastic Softening and Terminal Dispersions, of Linear Amorphous Polymers. *J. Polym. Sci. Part B: Polym. Phys. Ed.* **1986**, *24*, 619−632.
(88) Ngai, K. L.; Plazek, D. J. *Physical Properties of Polymers Handbook*, Mark, J. E., Ed.; American Institute of Physics: Woodbury, NY, 1996; Chapter 25, p 341.
(89) Schmidt-Rohr, K.; Spiess, H. W. Nature of Nonexponential Loss of Correlation above the Glass Transition Investigated by Multidimensional NMR. *Phys. Rev. Lett.* **1991**, *66*, 3020.
(90) Weeks, E. R.; Crocker, J. C.; Levitt, A. C.; Schofield, A.; Weitz, D. A. Three-dimensional direct imaging of structural relaxation near the colloidal glass transition. *Science* **2000**, *287*, 627−631.
(91) Donati, C.; Glotzer, S. C.; Poole, P. H.; Kob, W.; Plimpton, S. J. Spatial correlations of mobility and immobility in a glass-forming Lennard-Jones liquid. *Phys. Rev. E* **1999**, *60*, 3107.
(92) Tarjus, G.; Kivelson, D. SuperArrhenius character of supercooled glass-forming liquids. *J. Chem. Phys.* **1995**, *103*, 3071−3073.
(93) Chang, I.; Sillescu, H. Heterogeneity at the Glass Transition: Translational and Rotational Self-Diffusion. *J. Phys. Chem. B* **1997**, *101*, 8794−8801.
(94) Stillinger, F. H.; Hodgdon, J. A. Translation-rotation paradox for diffusion in fragile glass-forming liquids. *Phys. Rev. E* **1994**, *50*, 2064−2068.
(95) Hall, D. B.; Dhinojwala, A.; Torkelson, J. M. Translation-Rotation Paradox for Diffusion in Glass-Forming Polymers: The Role of the Temperature Dependence of the Relaxation Time Distribution. *Phys. Rev. Lett.* **1997**, *79*, 103−106.
(96) Ngai, K. L. Alternative Explanation of the Difference between Translational Diffusion and Rotational Diffusion in Supercooled Liquids. *J. Phys. Chem. B* **1999**, *103*, 10684−10694.
(97) Richert, R.; Duvvuri, K.; Duong, L. J. Dynamics of glass-forming liquids. VII. Dielectric relaxation of supercooled tris-naphthylbenzene, squalane, and decahydroisoquinoline. *J. Chem. Phys.* **2003**, *118*, 1828.
(98) Zhu, X. R.; Wang, C. H. Homodyne photon-correlation spectroscopy of a supercooled liquid: 1,3,5-Tri-α-naphthyl benzene. *J. Chem. Phys.* **1986**, *84*, 6086.
(99) Zemke, K.; Schmidt-Rohr, K.; Magill, J. H.; Sillescu, H.; Spiess, H. W. Molecular dynamics near the glass transition. *Mol. Phys.* **1993**, *80*, 1317−1330.
(100) Richert, R. On the dielectric susceptibility spectra of supercooled *o*-terphenyl. *J. Chem. Phys.* **2005**, *123*, 154502.
(101) Rajian, J. R.; Huang, W.; Richert, R.; Quitevis, E. L. Enhanced translational diffusion of rubrene in sucrose benzoate. *J. Chem. Phys.* **2006**, *124*, No. 014510.
(102) Kumar, S. K.; Szamel, G.; Douglas, J. F. Nature of the breakdown in the Stokes-Einstein relationship in a hard sphere fluid. *J. Chem. Phys.* **2006**, *124*, 214501.
(103) Chong, S.-H.; Kob, W. Coupling and Decoupling between Translational and Rotational Dynamics in a Supercooled Molecular Liquid. *Phys. Rev. Lett.* **2009**, *102*, No. 025702.
(104) Ediger, M. D.; Harrowell, P. Perspective: Supercooled liquids and glasses. *J. Chem. Phys.* **2012**, *137*, No. 080901.
(105) Ngai, K. L. The vestige of many-body dynamics in relaxation of glass-forming substances and other interacting systems. *Philos. Mag.* **2007**, *87*, 357−370.
(106) Chakrabarti, D.; Bagchi, B. Decoupling Phenomena in Supercooled Liquids: Signatures in the Energy Landscape. *Phys. Rev. Lett.* **2006**, *96*, No. 187801.
(107) Ngai, K. L.; Rendell, R. W. The Symmetric and Fully Distributed Solution to a Generalized Dining Philosophers Problem. In *Relaxation in Complex Systems and Related Topics*; Campbell, I. A.; Giovannella, C., Eds.; Plenum Press: New York, 1990; pp 309−316.
(108) Zhang, W.; Brian, C. W.; Yu, L. Fast Surface Diffusion of Amorphous o-Terphenyl and Its Competition with Viscous Flow in Surface Evolution. *J. Phys. Chem. B* **2015**, *119*, 5071−5078.
(109) Whitaker, K. R.; Scifo, D. J.; Ediger, M. D.; Ahrenberg, M.; Schick, C. Highly Stable Glasses of cis-Decalin and cis/trans-Decalin Mixtures. *J. Phys. Chem. B* **2013**, *117*, 12724−12733.
(110) Capaccioli, S.; Ngai, K. L.; Paluch, M.; Prevosto, D. Mechanism of fast surface self-diffusion of an organic glass. *Phys. Rev. E: Stat., Nonlinear, Soft Matter Phys.* **2012**, *86*, No. 051503.
(111) Cao, C. R.; Lu, Y. M.; Bai, H. Y.; Wang, W. H. High surface mobility and fast surface enhanced crystallization of metallic glass. *Appl. Phys. Lett.* **2015**, *107*, 141606.
(112) Ngai, K. L.; Capaccioli, S.; Cao, C. R.; Bai, H. Y.; Wang, W. H. Quantitative explanation of the enhancement of surface mobility of the metallic glass $Pd_{40}Cu_{30}Ni_{10}P_{20}$ by the Coupling Model. *J. Non-Cryst. Solids.* **2017**, *463*, 85−89.
(113) Zhang, Y.; Potter, R.; Zhang, W.; Fakhraai, Z. Using tobacco mosaic virus to probe enhanced surface diffusion of molecular glasses. *Soft Matter.* **2016**, *12*, 9115−9120.
(114) Zhang, Y.; Fakhraai, Z. Invariant Fast Diffusion on the Surfaces of Ultrastable and Aged Molecular Glasses. *Phys. Rev. Lett.* **2017**, *118*, No. 066101.
(115) Zhang, Y.; Fakhraai, Z. Decoupling of surface diffusion and relaxation dynamics of molecular glasses. *Proc. Natl. Acad. Sci. U.S.A.* **2017**, *114*, 4915−4919.
(116) Ngai, K. L.; Paluch, M.; Rodriguez-Tinoco, C. Why is surface diffusion the same in ultrastable, ordinary, aged, and ultrathin molecular glasses? *Phys. Chem. Chem. Phys.* **2017**, *19*, 29905.
(117) Ngai, K. L.; Capaccioli, S. Reconsidering the relation of the JG β-relaxation to the α-relaxation and surface diffusion in ethylcyclohexane. *J. Non-Cryst. Solids X* **2021**, *11*−*12*, No. 100070.
(118) Ngai, K. L.; Paluch, M.; Rodriguez-Tinoco, C. Why is the change of the Johari−Goldstein β-relaxation time by densification in ultrastable glass minor? *Phys. Chem. Chem. Phys.* **2018**, *20*, 27342.
(119) Swallen, S. F.; Kearns, K. L.; Mapes, M. K.; Kim, Y. S.; McMahon, R. J.; Ediger, M. D.; Wu, T.; Yu, L.; Satija, S. Organic Glasses

https://doi.org/10.1021/acs.jpcb.4c03520
J. Phys. Chem. B 2024, 128, 10709−10726

with Exceptional Thermodynamic and Kinetic Stability. *Science* **2007**, *315*, 353.
(120) Ishii, K.; Nakayama, H.; Hirabayashi, S.; Moriyama, R. Anomalously high-density glass of ethylbenzene prepared by vapor deposition at temperatures close to the glass-transition temperature. *Chem. Phys. Lett.* **2008**, *459*, 109−112.
(121) Leon-Gutierrez, E.; Sepúlveda, A.; Garcia, G.; Clavaguera-Mora, M. T.; Rodríguez-Viejo, J. Stability of thin film glasses of toluene and ethylbenzene formed by vapor deposition: an in-situs nano-calorimetric study. *Phys. Chem. Chem. Phys.* **2010**, *12*, 14693−14698.
(122) Whitaker, K. R.; Tylinski, M.; Ahrenberg, M.; Schick, C.; Ediger, M. D. Kinetic stability and heat capacity of vapor-deposited glasses of o-terphenyl. *J. Chem. Phys.* **2015**, *143*, No. 084511.
(123) Rodríguez-Tinoco, C.; Gonzalez-Silveira, M.; Ràfols-Ribé, J.; Garcia, G.; Rodríguez-Viejo, J. Highly stable glasses of celecoxib: Influence on thermo-kinetic properties, microstructure and response towards crystal growth. *J. Non-Cryst. Solids* **2015**, *407*, 256−261.
(124) Rodríguez-Tinoco, C.; Gonzalez-Silveira, M.; Barrio, M.; Lloveras, P.; Tamarit, J. L.; Garden, J.-L.; Rodríguez-Viejo, J. Ultrastable glasses portray similar behaviour to ordinary glasses at high pressure. *Sci. Rep.* **2016**, *6*, 34296.
(125) Ediger, M. D. Perspective: Highly stable vapor-deposited glasses. *J. Chem. Phys.* **2017**, *147*, 210901.
(126) Berthier, L.; Ediger, M. D. How to "measure" a structural relaxation time that is too long to be measured? *J. Chem. Phys.* **2020**, *153*, No. 044501.
(127) Lubchenko, V.; Wolynes, P. G. Theory of structural glasses and supercooled liquids. *Annu. Rev. Phys. Chem.* **2007**, *58*, 235.
(128) Stevenson, J. D.; Wolynes, P. G. On the surface of glasses. *J. Chem. Phys.* **2008**, *129*, 234514.
(129) Mirigian, S.; Schweizer, K. S. Unified theory of activated relaxation in liquids over 14 decades in time. *J. Phys. Chem. Lett.* **2013**, *4*, 3648.
(130) Mirigian, S.; Schweizer, K. S. Elastically cooperative activated barrier hopping theory of relaxation in viscous fluids. I. General formulation and application to hard sphere fluids. *J. Chem. Phys.* **2014**, *140*, 194506.
(131) Mirigian, S.; Schweizer, K. S. Elastically cooperative activated barrier hopping theory of relaxation in viscous fluids. II. Thermal liquids. *J. Chem. Phys.* **2014**, *140*, 194507.
(132) Mirigian, S.; Schweizer, K. S. Communication: Slow relaxation, spatial mobility gradients, and vitrification in confined films. *J. Chem. Phys.* **2014**, *141*, 161103.
(133) Mirigian, S.; Schweizer, K. S. Theory of activated glassy relaxation, mobility gradients, surface diffusion, and vitrification in free standing thin films. *J. Chem. Phys.* **2015**, *143*, 244705.
(134) Ngai, K. L. Relation between some secondary relaxations and the α relaxations in glass-forming materials according to the coupling model. *J. Chem. Phys.* **1998**, *109*, 6982.
(135) Ngai, K. L.; Paluch, M. Classification of secondary relaxation in glass-formers based on dynamic properties. *J. Chem. Phys.* **2004**, *120*, 857−873.
(136) Capaccioli, S.; Paluch, M.; Prevosto, D.; Wang, L.; Ngai, K. L. Many-body nature of relaxation processes in glass-forming systems. *J. Phys. Chem. Lett.* **2012**, *3*, 735−743.
(137) Ngai, K. L.; Paluch, M. Corroborative evidences of TV^{γ}-scaling of the α-relaxation originating from the primitive relaxation/JG β relaxation. *J. Non-Cryst. Solids* **2017**, *478*, 1−11.
(138) Mandanici, A.; Huang, W.; Cutroni, M.; Richert, R. Dynamics of glass-forming liquids. XII. Dielectric study of primary and secondary relaxations in ethylcyclohexane. *J. Chem. Phys.* **2008**, *128*, 124505.
(139) Mandanici, A.; Huang, W.; Cutroni, M.; Richert, R. On the features of the dielectric response of supercooled ethylcyclohexane. *Philos. Mag.* **2008**, *88*, 3961−3971.
(140) Mandanici, A.; Cutroni, M. A trace of the Johari−Goldstein relaxation in the mechanical response of supercooled ethylcyclohexane? *Mater. Sci. Eng. A* **2009**, *521*−*522*, 279−282.
(141) Ramos, S. L. L. M.; Ogino, M.; Oguni, M. Calorimetric distinction between the inter- and intra-molecular rearrangement processes in alkylcyclohexane liquids by means of spatial confinement. *J. Mol. Liq.* **2020**, *311*, No. 113359.
(142) Li, X.; Wang, M.; Liu, R.; Ngai, K. L.; Tian, Y.; Wang, L.-M.; Capaccioli, S. Secondary relaxation dynamics in rigid glassforming molecular liquids with related structures. *J. Chem. Phys.* **2015**, *143*, 104505.
(143) Rodriguez-Tinoco, C.; Ngai, K. L.; Rams-Baron, M.; Rodriguez-Viejo, J.; Paluch, M. Distinguishing different classes of secondary relaxations from vapour deposited ultrastable glasses. *Phys. Chem. Chem. Phys.* **2018**, *20*, 21925−21933.
(144) Kasting, B. J.; Beasley, M. S.; Guiseppi-Elie, A.; Richert, R.; Ediger, M. D. Relationship between aged and vapor-deposited organic glasses: Secondary relaxations in methyl-*m*-toluate. *J. Chem. Phys.* **2019**, *151*, 144502.
(145) Goldstein, M. The past, present, and future of the Johari−Goldstein relaxation. *J. Non-Cryst. Solids* **2011**, *357*, 249−255.
(146) Jin, X.; Guo, Y.; Feng, S.; Capaccioli, S.; Ngai, K. L.; Wang, L.-M. Isochronal superposition of the structural α-relaxation and invariance of its relation to the β-relaxation to changes of thermodynamic conditions in methyl m-toluate. *J. Phys. Chem. B* **2020**, *124*, 6690−6697.
(147) Prevosto, D.; Capaccioli, S.; Lucchesi, M.; Rolla, P. A.; Ngai, K. L. Does the entropy and volume dependence of the structural α-relaxation originate from the Johari−Goldstein β-relaxation? *J. Non. Cryst. Solids* **2009**, *355*, 705−711.
(148) Ngai, K. L.; Habasaki, J.; Prevosto, D.; Capaccioli, S.; Paluch, M. Thermodynamic scaling of α-relaxation time and viscosity stems from the Johari-Goldstein β-relaxation or the primitive relaxation of the coupling model. *J. Chem. Phys.* **2012**, *137*, No. 034511.
(149) Johari, G. P.; Goldstein, M. Viscous Liquids and the Glass Transition. II. Secondary Relaxations in Glasses of Rigid Molecules. *J. Chem. Phys.* **1970**, *53*, 2372.
(150) Goldstein, M. Communications: Comparison of activation barriers for the Johari−Goldstein and alpha relaxations and its implications. *J. Chem. Phys.* **2010**, *132*, No. 041104.
(151) Stevenson, J. D.; Wolynes, P. G. A universal origin for secondary relaxations in supercooled liquids and structural glasses. *Nat. Phys.* **2010**, *6*, 62−68.
(152) Casalini, R.; Roland, C. M. Aging of the Secondary Relaxation to Probe Structural Relaxation in the Glassy State. *Phys. Rev. Lett.* **2009**, *102*, No. 035701.
(153) Ngai, K. L.; Wang, L.-M.; Yu, H. B. Relating Ultrastable Glass Formation to Enhanced Surface Diffusion via the Johari−Goldstein β-Relaxation in Molecular Glasses. *J. Phys. Chem. Lett.* **2017**, *8*, 2739−2744.

https://doi.org/10.1021/acs.jpcb.4c03520
J. Phys. Chem. B 2024, 128, 10709−10726